Basics and applications of cryopumps

C. Day

Forschungszentrum Karlsruhe, Institute of Technical Physics, 76344 Eggenstein-Leopoldshafen, Germany

Abstract

This report introduces the wide field of cryogenic pumping, from commercial cryogen-free refrigerator cryopumps to very special, tailor-made cryopumps. It starts with a short historic overview of the field of cryopumping. Then, the principles of cryogenic pumping via sublimation/condensation and physisorption are introduced, and we illustrate how they are exploited to derive a design for a usable cryopump. In the third part, typical characteristics of cryosorption pumps are discussed. The report finishes with a few examples of applications.

1   Introduction

This report is aimed at giving a general overview of cryopumping. Usually, the cooled surface is at least partly covered with a porous sorbent material. The design of a cryopump has to combine cryogenic aspects and technological vacuum considerations in a unique manner, as the generation of low temperature itself presupposes the existence of vacuum conditions and vice versa. Thus, the cryopump is by its physical principle a high-vacuum pump. Besides straightforward parameters, such as pressure and temperature, the performance cryopump is very much governed by the complex interaction between gas particles and cooled sorbent surface, which will be discussed in detail in this report. The cryopump is the pump type that provides the highest pumping speeds, especially when operated in situ of the vacuum recipient.

The present report contains an extensive list of references, a mixture of textbooks and specialized articles, to provide the reader with the opportunity to pursue any further details he might be interested in.

2   History of cryopumping

Not surprisingly, the development of cryopumping went in parallel with the advances made in liquefaction (liquid nitrogen, 77.3 K, Dewar, 1874; liquid hydrogen 20.4 K, Dewar, 1898; liquid helium, 4.2 K, Kammerlingh Onnes, 1908). It was soon found that vacuum can be produced by charcoal kept at these cryogenic temperatures. The successful use of liquid-nitrogen-cooled traps to prevent oil backstreaming from diffusion pumps was reported in the 1910s by Gaede and Langmuir.

However, the first large-scale applications of cryopumping were triggered by the first space projects in the 1950s. They often included operation with liquid hydrogen. In the second half of the last century, liquid helium bath-cooled cryopumps were very popular for laboratory applications, when oil contamination was requested (so that diffusion pumps could not be used) and manual re-fill was not a problem.

The next big step forward was the development of cryogen-free regenerative refrigerators by Gifford and McMahon in 1960. These devices have seen a significant progress towards higher cooling power at lower end temperatures, and their development continues.

Nowadays, Gifford–McMahon cooled cryopumps are the high-vacuum pump of choice in many industrial processes, such as the semiconductor industries, especially in the USA. The company CTI-Cryogenics (now with Brooks Automation Inc.) is the leading global cryopump manufacturer. In Europe, turbomolecular pumps have widely replaced cryopumps in vacuum process plants.

3   Cryopumping fundamentals

By international classification, a cryopump is defined as a vacuum pump which captures the gas by surfaces cooled to temperatures below 120 K [1]. To achieve vacuum in a closed volume means, simply speaking, to remove all molecules in the gaseous phase within this volume. According to the different physical principles, which are exploited to create, improve or maintain vacuum, there are different types:

– Positive displacement or mechanical pumps, which provide volumes to be filled with the gas being pumped. The volumes are cyclically isolated from the inlet, the gas is then transferred to the outlet. In most types of positive displacement vacuum pumps the gas is compressed to atmosphere before the discharge at the outlet. Positive displacement pumps work independently of the gas species to be pumped.

– Kinetic pumps, which impart momentum to the gas being pumped in such a way that the gas is transferred continuously from the pump inlet to the outlet.

– Entrapment or capture vacuum pumps, which retain gas molecules by chemical or physical interaction on their internal surfaces.

Together with the getter and the sputter ion pump, the cryopump is the most prominent representative of the latter group. As for all high vacuum pumps (i.e., pumps working below the 10^{-3} Pa range) an appropriate medium forepressure has to be provided by a mechanical forepump, before the cryopump can be started. The forepump is also needed to exhaust the gas to the atmosphere. Whereas this gas transfer is done continuously in the case of kinetic and positive displacement pumps, entrapment pumps do this in a batch-wise manner as they accumulate the gas during pumping and must be regenerated from time to time. During actual pumping, the gases within the entrapment pump systems are instantaneously immobilized and no outlet is required at all.

3.1   Cryopumping mechanisms

The cryopumping effect is produced by intimate interaction between the gas particles to be pumped and a cold surface provided to them in the cryopump. The forces involved are relatively weak (primarily van der Waals dispersion type) and do not include chemical bonds, as is the case for chemisorption with the chemically active alloys in getter pumps. Consequently, cryopumps do not require such high temperatures for regeneration. Cryopumps can pump all gases including noble gas, if the temperature is sufficiently low.

The amount of molecules that can be accumulated depends on a number of physical factors such as temperature of gas and surface, physicochemical properties of gas and surface (surface energy distribution), microscopic roughness of the surface, etc. The different categories are treated in the following sections.

3.1.1   Cryocondensation

In this case, the surfaces must be cooled to such a temperature as to keep the corresponding saturation pressure equal to or below the desired vacuum pressure in the chamber. The achievable pressure is determined by the saturation pressure at the temperature chosen for the cold surfaces. This principle is the most elementary of all forms of capture pumping. For many gases, the pressure range of

cryopumps is below the triple point pressure of the individual gases to be pumped. Thus, the relevant saturation curve becomes identical with the sublimation curve, i.e., during pumping, the gas particles undergo direct phase transition from the gaseous to the solid phase without any liquid phase. Within this report, as is customary in cryopumping, the term 'condensation' is used for both types of transition out of the gaseous phase, and combines re-sublimation (gaseous → solid) and condensation (gaseous → liquid). It must be noted that standard data libraries do not include the sublimation regime, but often have the triple point temperature as lower limit [2], as typical problems are encountered in the low temperature region. For example, the 'correct' vapour pressure values are only relevant for surface coverages greater than one monolayer [3, 4]. Thus, for use in the low temperature regime needed for cryopump design, carefully selected sources have to be quoted (^{3}He [5, 6], ^{4}He [7], hydrogen isotopes [8]). Figure 1 shows the sublimation equilibrium curves of some relevant gases. In principle any gas can be pumped, provided the surface temperature is low enough. It can be seen from this figure that neon, hydrogen isotopes, and helium require the lowest temperatures.
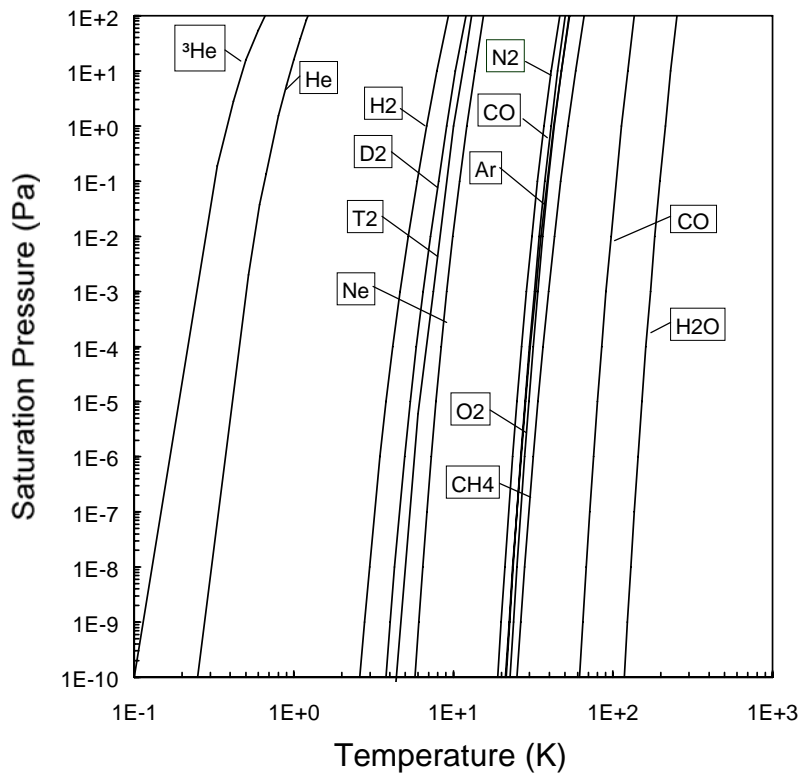

Fig. 1: Saturation curves of common gases

The temperature of about 100 K would be sufficient to condense water and all hydrocarbons, e.g., oil vapours. To condense the air components, the 20 K level is needed. The 4 K level is sufficient to condense the hydrogen isotopes and neon. By further reduction of the temperature, the ultra-high vacuum range (10^{-5} to 10^{-8} Pa) is fully accessible.

When using Fig. 1 as a basis for cryopump design, one must be aware that the saturation curve is associated with thermodynamic equilibrium at the phase boundary. This means a net particle flux of zero, or: zero pumping speed. For practical applications, it is recommended to provide for oversaturation of the gas by two orders of magnitude in pressure. Figure 2 exemplifies the consequences of that procedure. In order to establish a pressure of 10^{-4} Pa during pumping of H_2 (corresponding to an equilibrium temperature of 4.2 K), one needs to provide a cold surface temperature of 3.6 K (the equilibrium temperature of 10^{-6} Pa).
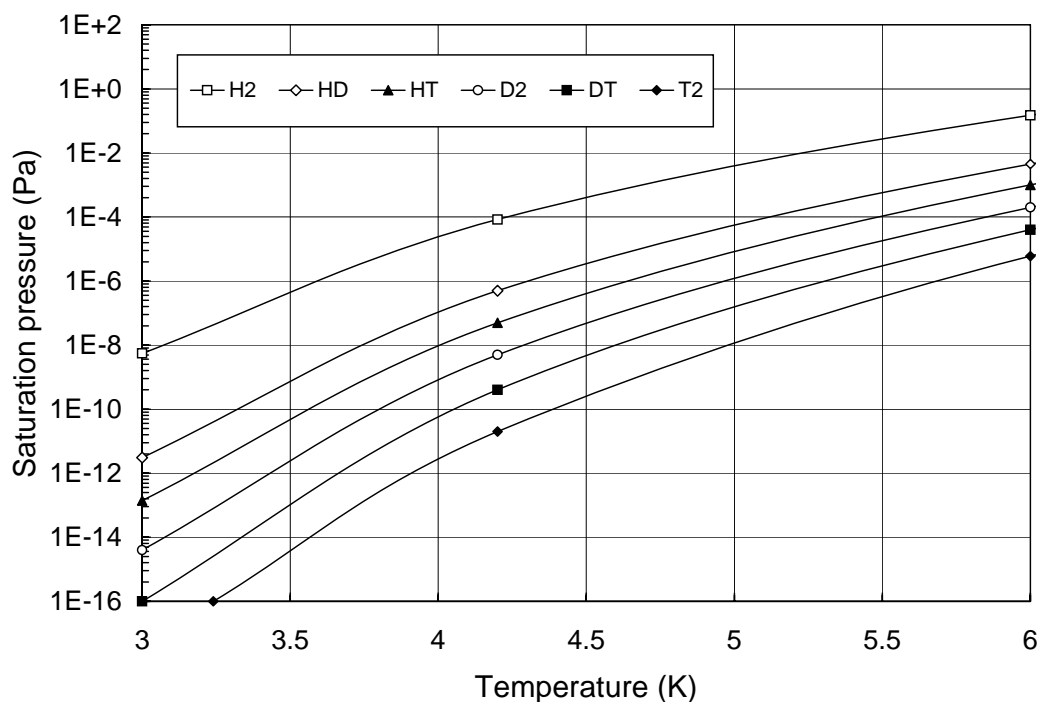
Fig. 2: Sublimation pressures of the six hydrogen isotopomers [8]

During cryocondensation, condensate layers are formed by crystal growth out of the gas phase. This growth process takes place over three stages: Firstly, thermal accommodation of the impinging particle and adsorption on the surface, then, diffusion to the growth site on the crystal lattice, and, thirdly, atomic incorporation. It has been shown that the second step governs the overall condensation velocity [9]. The efficiency of the condensation process is expressed by means of the condensation coefficient α_c, defined as the number of condensed particles related to the number of particles incident upon the cryosurface [10, 11]. Assuming high supersaturation, a condensation coefficient of unity is achievable without any problem. In most cases, the cryocondensation growth starts by forming one or a few monolayers and then changes to form islands on top of them. Thus, the cryodeposits obtained during pumping may be quite non-uniform. The growth of condensed layers is not limited in principle. But for regions with increased layer thickness, the surface temperature of the condensate rises, thus leading to higher surface mobility of the pumped particles. This results in a higher risk of spontaneous transpositions and should be avoided in any case.

3.1.2   *Cryosorption*

Gas particles impinging on a surface of sufficiently low temperature lose so much of their incident kinetic energy that they stay attached to the cold surface by weak intermolecular forces, resulting in significantly higher molecular concentration on the surface than in the gas phase. This phenomenon is called physical adsorption or physisorption. The reader interested in going into details is advised to check the pertinent textbooks on adsorption energies and theory on intermolecular forces [12–15]. Cryosorption denotes the physical adsorption process under vacuum conditions and low temperatures. The equilibrium pressure of adsorbed gas particles is significantly lower than the corresponding saturation pressure for cryocondensation. This is due to the fact that the dispersion forces between the gas molecule and the surface are greater than between the gas molecules themselves in the condensed state. Hence, gas can be retained by adsorption even in a subsaturated state, i.e., at considerably higher temperatures than would be required for condensation. This fact is essential in cryopumping helium, hydrogen, and neon, which are difficult to condense.

However, the cryosorption process is quite complex and very much determined by the actual nature of the surface (chemical, mechanical, physical), not only by its temperature, as is the case for cryocondensation. Porous materials with high sorption capacity, such as molecular sieves or activated carbons are most often used as sorbent materials. However, layers of condensed gas frost (Ar, CO_2, SF_6) may also be applied. The characteristic of cryosorption is given by the respective sorption isotherm. It is possible to bind helium or hydrogens in the 5 K temperature range and to achieve equilibrium pressures in the 10^{-7} Pa region without any problem. Figure 3 shows the typical sorption isotherm curves for helium, hydrogen and deuterium, which cannot be pumped by condensation at the standard available 4.2 K. As customary in adsorption technology, the sorbed amount is given in standard cm³ (referenced at 1 atm and 273.15 K), related to the sorbent mass. Contrary to condensation, where a simple saturation p–T plot is sufficient to estimate the performance (Figs. 1 and 2), cryosorption requires the knowledge of a 3-D relationship between p, T, and the sorbed amount.
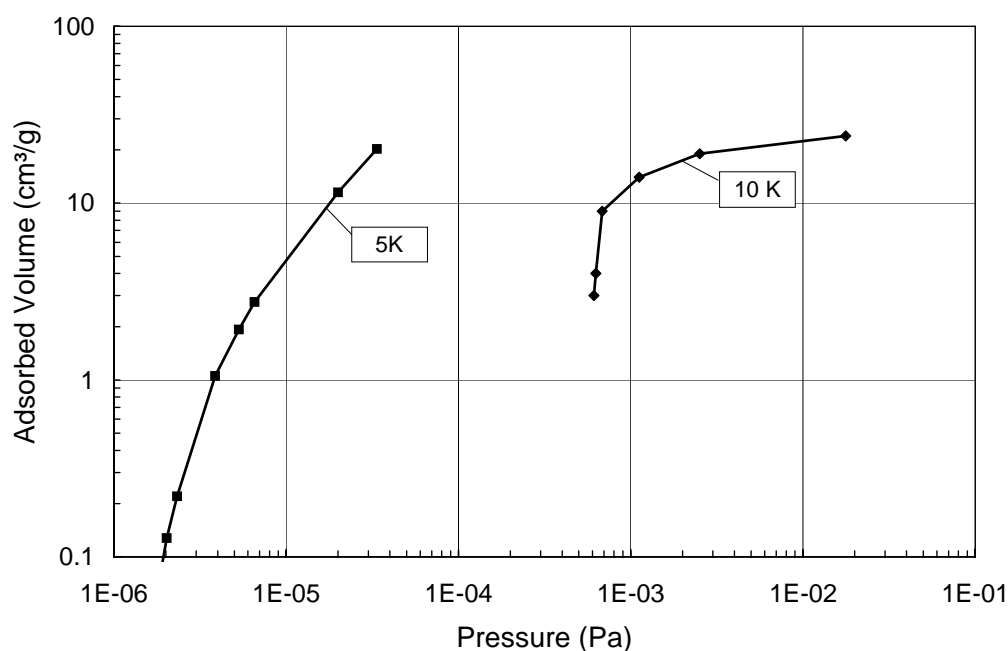

Fig. 3: Sorption equilibria for helium at a microporous activated charcoal

The sticking coefficient (the sorption analogy to the condensation coefficient), i.e., the number of molecules which are sorbed on a surface in a given interval of time divided by the number of molecules impinging on that surface, may be considerably below unity, depending on the material–gas pair. Due to the physical principle, cryosorption pumping is limited to some monolayers of gas coverage on the surface. Then the effect of the surface becomes negligible and the resulting pressure starts to increase rapidly.

3.1.3   Cryotrapping

This is the concurrent pumping of two or more gases by entrainment of gas particles which are not condensable at the prevailing temperatures and pressure conditions. For the purpose of entrainment, a condensing gas is used, so that a mixed condensate is formed. Usually, the small molecules of the gas to be pumped are caught in the open lattice of the cryodeposit of a more abundant species and are quickly buried by subsequent layers. As most of the bonded gas particles are occluded in the condensate layer and only a certain percentage directly interacts with the surface, the achievable equilibrium pressures are even lower than those achievable by cryosorption. The entrapment ratio (i.e., the number of pumped molecules of one species related to the number of deposited molecules of the

condenate species) is higher than with pumping by layers of pre-condensed frost (see, for example, pumping of He by condensed Ar). However, the main disadvantage of this technique is the additional gas input into the system which has to be evacuated. This helps during pumping, but has to be coped with during regeneration and, thus, requires larger forevacuum systems.

3.2 Heat load assessment

Cryopumping means the generation of vacuum by low temperatures. Thus, the generation and availability of low temperatures is a prerequisite for the operation of cryopumps. Cryogenics is dealt with in detail in a separate report of this summer school. Therefore, the following section is limited to the specific cryogenic aspects of cryopumping.

The cryopump housing will usually be at ambient temperature, whereas the cryopanel must be refrigerated. So, there will always be heat flux onto the panel due to the different temperatures. It is essential for establishing stably low temperatures to reduce heat influx on the cold surface. The total thermal load $\dot{Q}$ transmitted to the cryosurface consists of the sum of heat flow rates produced by thermal conductivity of the solids, gas heat conduction, and thermal radiation. For working cryopumps the thermal loads due to cryosorption and/or cryocondensation still have to be added. This results from the enthalpy change between particle temperature and phase transition temperature $\Delta\dot{H}_{cool}$, and the phase change enthalpy $\Delta\dot{H}_{Ph}$ itself:

$$\dot{Q} = \dot{Q}_S + \dot{Q}_G + \dot{Q}_R + \Delta\dot{H}_{cool} + \Delta\dot{H}_{Ph} \rightarrow \min . \tag{1}$$

Under steady-state conditions, the total heat load becomes equal to the refrigeration power by the cold source. At increasing inlet pressures, the load also increases and the immobilization gas load becomes predominant. The different contributions and the strategies of how to minimize them are an important issue in cryopump design.

3.2.1 Solid heat conduction

The heat transmitted by solid conduction (e.g., via piping and instrumentation, fastenings, supply lines, cables) is proportional to the cross-section A and the thermal conductivity λ at the applied temperature difference (between warm wall and cold surface), and inversely proportional to the conductor's length L:

$$\dot{Q}_S \sim \frac{\lambda}{L} \cdot A . \tag{2}$$

This energy input must be kept at an adequately low level by the constructional geometry and by the correct choice of materials. To avoid parasitic heat flows, stainless steel is a good material owing to its low conductivity. However, one has also to compromise the need for materials with high thermal conductivity at cryogenic temperatures (such as copper) to provide good thermal contact with the cold surface.

3.2.2 Gaseous heat conduction

The influence of residual heat conduction in the gas is due to the energy transfer within collisions between the molecules and any surface. This effect is associated with the mean free path, which denotes the average distance which a molecule travels between two successive collisions. It can be practically eliminated, when the mean free path Λ between two particle hits is considerably larger than the characteristic vessel dimension d, which begins to hold at lower pressures. In this case, the collisions between molecules become less frequent and the molecules collide predominantly with the

vessel walls. Then, the heat transfer depends only on the number of molecules and a linear relationship develops between gas heat conductivity and pressure. At higher pressures, the gaseous heat transfer is much higher and owing to convective bulk motion of the gas and the thermal conductivity of the gas does not change significantly with pressure.

To characterize this effect and for division into different regimes of flow, the Knudsen number is used, which is defined as the ratio of the mean free path to a characteristic dimension of the system (like, for example, the vessel diameter):

$$Kn = \frac{\Lambda}{d} .$$

(3)

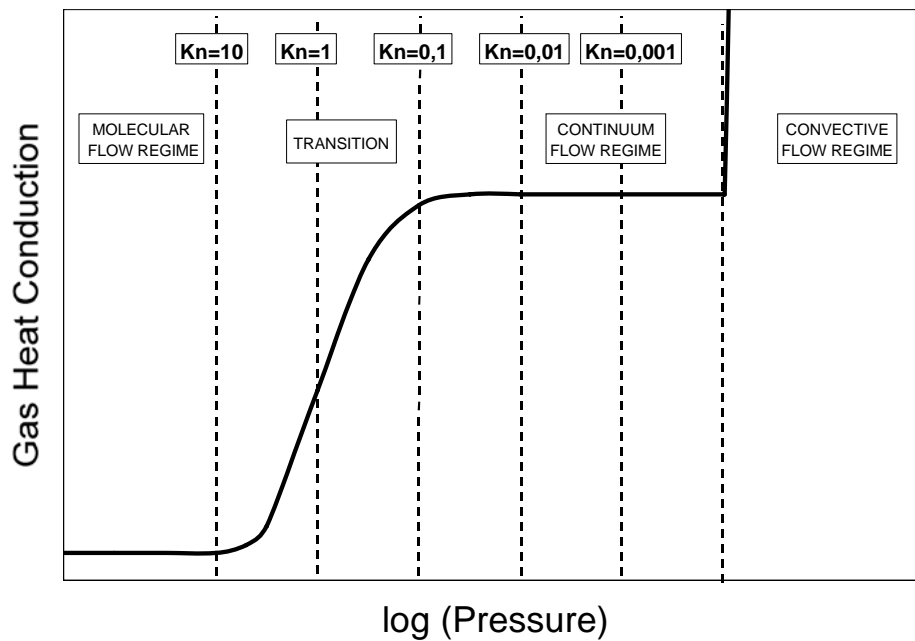According to Fig. 4, there are four regimes of gaseous heat transfer.

Fig. 4: Schematic gas heat conduction (arbitrary units) as a function of pressure at different *Kn* numbers

The regime with *Kn* >> 1 is called the molecular flow regime, where the influence of gas heat conduction can be neglected [16]. A cryopump is normally operated under molecular flow conditions. However, depending on the application, and especially for tailor-made cryopumps for which cryogenic supply is not the limiting factor, one may benefit from the fact that the pumping speed of the cryopump increases with decreasing *Kn* number [17]. Table 1 gives a hint as to what pressures are needed to establish molecular flow conditions for different gases at different temperatures.

Table 1: Gas pressures (in Pa) corresponding to *Kn* = 10 for a vessel with 1 m diameter

Temperature (K)	He	H_2	N_2	CO_2
300	1.9×10^{-3}	1.3×10^{-3}	6.7×10^{-4}	4.4×10^{-4}
80	4.4×10^{-4}	2.6×10^{-4}	1.1×10^{-4}	
4	1.2×10^{-5}	C O N D E N S A T I O N		

3.2.3 Radiative heat transfer

Under molecular flow conditions, radiant heat from the process side in the vacuum chamber and the pump body is the primary heat load on the panels. For a pump to be heated by radiation, there are two requirements. Firstly, the heat has to be emitted from the chamber, and, secondly, the pump must absorb the incident radiation. Both possibilities have to be minimized by an appropriate design.

The radiation heat exchange between two diffuse, grey surfaces A_1 and A_2 with emissivities ε_1 and ε_2, respectively (for example 1 is the chamber wall, 2 the cryosurface), is given by [18]:

$$\dot{Q}_{12} = C_{12} \cdot A_1 \cdot (T_1^4 - T_2^4) , \tag{4}$$

with the exchange number C_{12} given by:

$$C_{12} = \frac{\sigma \cdot \varepsilon_1 \cdot \varepsilon_2}{1 - (1 - \varepsilon_1) \cdot (1 - \varepsilon_2) \cdot \varphi_{21}} , \tag{5}$$

where $\sigma = 5.678 \times 10^{-8}$ W/(m$^2 \cdot$ K^4) is the Stefan-Boltzmann constant and φ denotes the view factor. The view factor (or shape factor) φ_{12} is defined as the fraction of the radiation leaving 1 that is intercepted by surface 2 and determined by the geometric situation only. The analytical treatment to assess these values is quite complicated, so compilations of these data are usually employed [18, 19], whenever possible. For complicated geometries, the (Test Particle) Monte Carlo method or the angular reflection coefficient method are very appropriate tools to calculate the thermal radiation heat transfer due to photons scattered on the existing obstructions in the pump [20, 21]. These types of calculations directly yield the (thermal) transmission coefficient t, which denotes the percentage of the total power of incident thermal radiation finally arriving at the cryosurface.

The minimization of radiation heat influx is usually done by reducing the emissivity ε_1 of the internal pump surface. By very clean electropolishing, emissivities of 0.01 are obtained. But this effect is often masked by water humidity adsorbed or condensed on the walls, which leads to radiation almost equal to black body radiation [22]. So, the thermal load on the cryosurface coming from the chamber walls at 300 K is still much too high. Therefore, the cryosurface is even more protected from the radiation heat load. To do that, an optically dense and blackened (emissivities ε greater 0.9), cooled radiation shield is installed around the cryopanel to adsorb the entering stray radiation from the vacuum chamber source. The thermal transmission coefficient t associated with such array structures is of the order of 0.01 [23]. By installing baffle structures, the resulting overall radiation onto the panel has two contributions. Firstly, the residual radiation from the walls at ambient temperature [reduced by factor $(\varepsilon_2 \cdot t)$], and, secondly, the direct radiation from the installed shields and baffle structures (at about 100 K). The disadvantage of any baffle from the vacuum pumping point of view, is a significant conductance reduction on the route of the particle from the cryopump inlet to the cryosurface (see Section 3.5). If the radiation heat load must be further decreased, the cryopump must be removed from the direct line of sight by designing some bends and elbows. But the main disadvantage of this method is that it again reduces conductance and the available net pumping speed.

The radiation shield is operated as a second cryopanel, but at a higher temperature level. In the entrance direction, the radiation shield is open, but constructed in such a way that no particle can traverse without colliding with the wall. Consequently, all gases impinge first on the cold baffle surface and become thermalized before reaching the actual cryosurface. This will already remove some high boiling gases by being pumped via cryocondensation on the baffle before they reach the sorbent. Thus, full capacity of the sorbent is available for removing the remaining gases. Good designs of the entrance baffle have to compromise efficient radiation shielding of the cold cryopanel with as high a conductance as possible for the incoming gas flow. Usually, louvre or chevron baffles are used, providing maximum (molecular) transmission probabilities w of about 40% and 25%, respectively [21, 24, 25].

3.2.4 Enthalpy transfer

During pumping, the cryopanel must absorb the energy of the incoming particles, i.e., the enthalpy difference for cool-down between baffle temperature and panel temperature and the energy connected with the phase change in the subsequent immobilization step. In this respect, the baffle is an essential help.

3.3 Cryopump types

In this section we address the different designs for cryopumps, which have been developed to meet the cryogenic and vacuum aspects discussed above. Each cryopump is made up of the three basic parts, namely, the entrance baffle, cryopanel and refrigeration unit. In most cases, the cryopanel is, at least partly, designed as a cryosorption panel. In the following, the cryopump designs are classified according to the cooling principle which is involved to cool the cryopanels.

3.3.1 Bath cryopumps

These cryopumps take the pattern of well-known dewar and cryostat designs. The pumping surfaces facing the vacuum vessel are directly cooled from their back side with liquid cryogens, i.e., boiling at ambient pressure, which are stored in dewar vessels. Thus, temperatures of 77.3 K (liquid nitrogen, LN), 27.1 K (liquid neon), 20.3 K (liquid hydrogen H_2), 4.2 K (liquid helium LHe) can be attained. The pumping surface in any case has to be shielded by a LN-cooled stage against thermal radiation.

To achieve long holding times with continuous operation, an automatic refill device must be used. To achieve further fractionation of the gases to be pumped, the 4 K LHe cryosorption panel may be shielded by an additional baffle, which is also cooled with LHe. In this three-stage version, a 80 K (LN temperature) condensation stage is obtained for high molecular gases, a 4 K condensation stage for all remaining gases passing the 80 K stage except for helium and hydrogen, and the final 4 K cryosorption stage. However, the overall conductance of such a configuration is reduced. The typical set-up of such a cryopump is shown in Fig. 5.
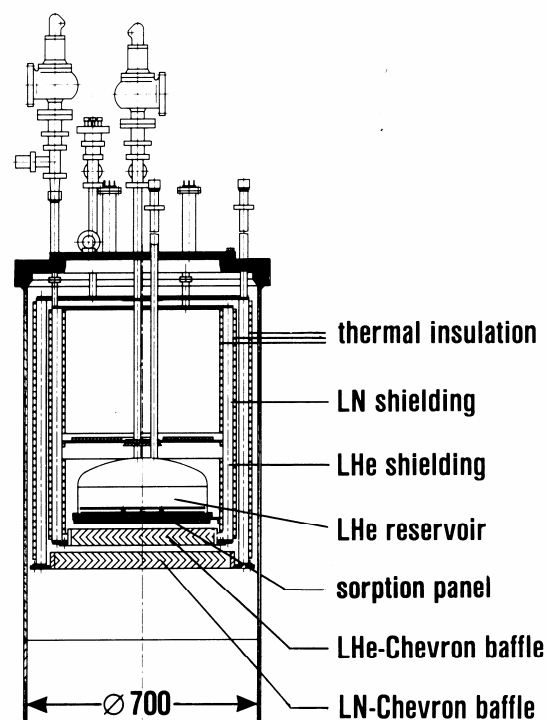

Fig. 5: Typical set-up of a bath cryopump in three-stage configuration. The LHe baffle is removable to obtain a two-stage configuration.

On account of clumsiness in handling liquid cryogens and the high capital and operational costs involved, bath-cooled cryopumps, with a few notable exceptions, are nowadays almost exclusively used in research laboratories and to a great extent replaced by refrigerator-cooled cryopumps which are described in the following.

3.3.2 *Refrigerator-cooled cryopumps*

Most modern cryopumps today are cooled by closed-loop mechanical refrigerators, using helium as a working fluid. Nowadays, refrigerator-cooled cryopumps are almost exclusively based on the two-stage Gifford and McMahon (GM) process [26, 27]. The gaseous helium is circulated continuously between a compressor and an expander, which are connected via flexible hoses. Two stages of these machines are required to achieve temperatures low enough to pump all gases except neon, helium, and hydrogen by cryocondensation. The first stage usually operates in the range of 50 to 75 K. It is used to cool the structures that provide for the radiation shielding and cools the baffles across the inlet of the pump. The second stage, which usually operates at about 10 K, is used to cool the inner cryopanel that is used to immobilize the gases which pass the baffle structures. Often, the second stage is covered with a sorbent material (at the back side) to allow for cryosorption pumping.
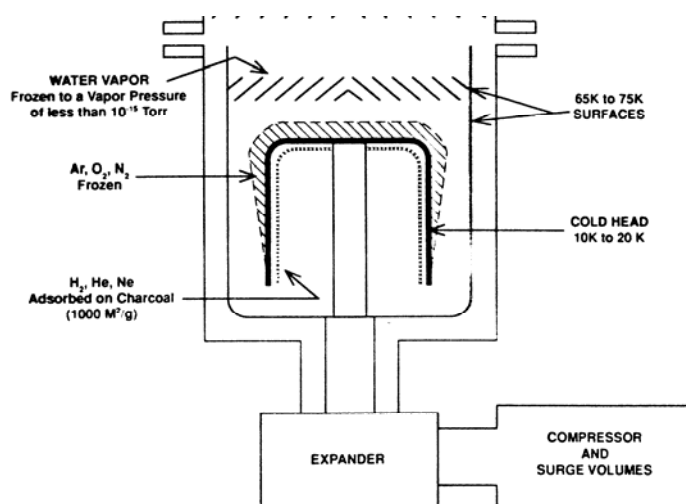

Fig. 6: Typical set-up of a two-stage refrigerator-cooled cryopump

Fig. 7: Cryopumps of the 3000 l/s class: Oerlikon Leybold Coolvac 3000 (left) and CTI On-Board 10 right)

As the refrigeration power for the regenerative cryoprocesses is limited, they are used as small-size cryopumps. From a pragmatic point of view the practical cross-section is often given by the availability of an appropriate upstream valve, which is difficult/expensive for sizes above DN250CF. Nevertheless, GM cryopumps at moderate size have been installed in many industrial processes in the semiconductor and coating industries [28, 29]. A typical set-up is shown in Fig. 6. Figure 7 gives two photos of commercially available pumps.

In former years, the pumping speed for He was very low, as the lowest temperature at the second stage was about 8–10 K, at which temperature the sticking coefficient of He on charcoal is too small. However, this disadvantage has been overcome within the last decade; excellent progress has been made in extending the available temperature range at the second stage to lower temperatures by integration of new rare-earth regenerator materials into the cold heads, providing up to 2 W at 4 K. The system-inherent vibration of refrigerator-cooled cryopumps, which has been detected to be a problem for some severe applications in nanotechnology, can be handled by sophisticated set-ups [30].

The refrigerator-cooled pumps are easy to apply and allow for an easy and complete automation of the pumping process, as storage or transfer systems for liquid cryogens are no longer needed. Standard off-the-shelf cryopumps have been available since the mid 1980s, with nominal aperture diameters of up to 1000 mm (e.g., for equipment of space simulation chambers). Technical data of a typical representative are listed in Table 2 (see also Section 3.4.2 for explanation of the categories). It becomes obvious that, even though pumping speed data for helium are comparable to those of other gases, the capacity is smaller by two orders of magnitude and, hence, becomes one of the pump's performance limits.

Table 2: Listed performance data (average taken from the catalogue of different manufacturers) for a typical 3000 l/s class two-stage GM cryopump

Parameter	Value
Pumping speed (l/s) water	9000–10500
Air	3000–3250
Hydrogen	4500–5200
Argon	2500–2700
Helium	1500–2300
Maximum throughput (Pa·m³/s) argon	1.0–2.5
Hydrogen	1.2
Pumping capacity (Pa·m³) argon	1.5×10^5–3×10^5
Hydrogen	1500–5000
Helium	10–100
Ultimate pressure (N_2 equivalent) (Pa)	$10^{-9} - 10^{-10}$
Cool-down time (h)	1.5–2.5
Crossover (Pa·m³)	35–50
Weight (kg)	30–50

3.3.3 *Supercritical helium-cooled cryopumps*

In this class of cryopumps the cryosurface is cooled with a continuous flow of cold helium, pressurized to supercritical pressures (such as 0.4 MPa). By appropriately selected heat exchangers to warm up the 4 K helium gas, all temperatures are adjustable. These cryopumps are recommended in cases where large helium reservoirs are available anyhow, as, for example, in a number of large-scale scientific research areas, like space simulation chambers, particle accelerators and storage rings, or thermonuclear fusion experiments.

3.3.4 *Alternative cryopump concepts*

The development of novel cryogenic pump concepts is a vital field of continuous efforts. Some promising concepts are mentioned below. Shigi tried to improve the drawbacks of the turbomolecular pump performance with respect to limited pumping speed for water and back-diffusion of hydrocarbon vapours by adding a cryogenically cooled baffle to the turbopump [31]. Perin *et al*. at CEA, France, continued the development of a turbomolecular pump under cold conditions, involving cryocoolers but without any sorbent stage [32]. Hemmerich used the diffusion pump principle [33]. His cryopump is successfully in use in the JET Tokamak, Culham, UK. For cyclotron vacuum chambers, a special heat transfer concept between the refrigerators and the cryopanel based on cryogenic heat pipes was developed and installed [34]. Foster developed an Ar frost based cryopump with a special device to regenerate the cryosurfaces; this pump can be operated continuously as the cryodeposits are removed mechanically by a snail head riding over the cryopanel surface [35].

3.4 Cryopump performance parameters

3.4.1 *Choice of cryosorbent*

Depending on the actual pumping task, a pure condensation pump without any sorbent may be fully sufficient. However, at the temperature level of ~ 4 K, which is the minimum level for standard cryopumps (cooled by liquid helium, or refrigerator-cooled), cryosorption is needed to pump helium; helium pumping is a function that is favourable to have, because helium is the standard gas used for leak detection. Moreover, the great improvement of using cryosorbent materials against cryocondensation is due to the achievement of much smaller equilibrium pressures. As the effect of cryosorption pumping is surface-generated, it tends to vanish with increasing surface coverage. Therefore, candidate materials must provide very high internal surfaces to have enough sorption capacity. The physical characterization of a porous sorbent material involves parameters such as

- geometry (granules, powder, spheres, pellets, fibres) and particle size distribution,

- surface structure,

- density,

- total specific surface area,

- pore size distribution and from that pore specific volume and mean pore size,

- pore shape.

The three latter aspects can be derived from measured sorption isotherms. Under high vacuum and small load conditions it is often justified to use very simple expressions for the isotherms.

The simplest adsorption isotherm is Henry's law, in which the amount of adsorbed gas Q varies linearly with the pressure (cf. Fig. 3):

$$Q = c \cdot p , \tag{6}$$

with *c* being the proportionality constant. This equation holds in the boundary case of perfect gases with no interactions between the adsorbed gas molecules (however, all correct model equations should possess the Henry dependency at the low end of the pressure range).

Another equation which is often used for cryosorption is the empirical Freundlich isotherm

$$Q = c \cdot p^{1/n}. \tag{7}$$

It is known that the cryosorption properties of a sorbent do not linearly correlate just with the total surface area (usually between 1000 m²/g and 2000 m²/g): the pore size distribution is the more fundamental property [36]. The pore width denotes the characteristic diameter of a pore, e.g., the diameter of a cylindrical pore. It is customary to differentiate between [37, 38]

- ultramicropores: pore width < 0.7 nm,

- supermicropores: pore width between 0.7 and 2 nm,

- mesopores: pore width between 2 and 50 nm,

- macropores: pore width > 50 nm.

The most popular technique for characterization of porous solids by means of the sorption isotherm is based on the 77 K nitrogen isotherm. The two most interesting properties to derive from experimental sorption isotherms are the pore-size distribution and the surface area *A* of the solid, for which there exist standard procedures, based on the isotherm model of Brunauer, Emmett and Teller (BET) [39]. However, the BET model is not applicable to microporous solids, which is the material of choice for cryopumping. Consequently, the total surface area can only be regarded as a fingerprint for intercomparison. One should be very careful to take these values as real. Moreover, this procedure is based on the interrelation of nitrogen molecules with the pores at 77 K. It is easy to understand that the situation may be very different for hydrogen at 20 K, or helium at 4 K. Therefore, in most cases, the choice of a cryosorbent material must be supported by characterization experiments.

In the literature, several programmes have been carried out to investigate and benchmark the suitability of different materials for use in cryosorption pumping. They all originated from world-wide R&D programmes launched in the early 1990s for nuclear fusion development. Perinić and co-workers at Forschungszentrum Karlsruhe, Germany, performed extensive comparative sorption screening tests involving materials such as sintered metal, porous ceramics, metal fibre fleece, alumina, silica gel, zeolite (molecular sieve), activated carbon and condensed Ar frost [40–42]. A parallel benchmark study was carried out at Los Alamos, USA, by Sedgley *et al.* [43–47]. Similar work, including thin metal films was done at the Efremov-Institute in Russia by Gurevich and co-workers [48, 49]. The use of metal structures as cryosorbent has successfully been demonstrated [50–52]. Recently, carbon fibres have been characterized for the LHC at CERN [53, 54]. However, the three sorbent types zeolite, activated carbon and condensed gas are the most important representatives and they will be treated in detail in this section. It was unanimously revealed that activated charcoal, especially of the coconut type, exhibits the best dynamic performance characteristics.

A special aspect of the benchmark tests was the determination of the optimum bonding technique to fix the sorbent on a flat panel structure. The influence of the material used for attachment was investigated comprehensively (mechanical fastenings, organic cements (epoxy resins), inorganic cements (silicate, metallic), braze bonding, soldering, plasma spraying) [42, 43, 49], but the results found differed very strongly. Thus, it is believed that this influence is very much due to the manufacturing know-how available and it will therefore not be discussed broadly in this report. One must ensure that the material used for bondage is compatible with UHV conditions and does not

produce outgassing problems. In almost all commercial cryopumps with sorption stage, activated charcoal is used as sorbent and it is bonded to the cryopanel by means of epoxy resins. At Forschungszentrum Karlsruhe, a special technique based on an inorganic cement was developed within the fusion programme, characterized in much detail as reference solution for ITER, and successfully employed in several tailor-made large-scale cryopumps [55].

3.4.1.1   Zeolite molecular sieves

Zeolites are hydrated aluminosilicates with well-defined structures. In most cases they are produced synthetically and their properties may be fine-tuned by the ratio of cations and anions; natural zeolites are formed from the alteration of volcanic ash. A wealth of different zeolites are used commercially because of their unique adsorption, catalytic, and ion-exchange properties. Because of their regular and reproducible structure they behave in a very predictable fashion, based on the defined monodisperse pore size distribution which relates strongly with the kinetic diameter of the molecule to be adsorbed. Therefore they can work as molecular sieves, allowing smaller molecules in while excluding larger ones.

Numerous papers have been published on the use of 3 Å, 4 Å, and 5 Å zeolite as filling material of sorption columns. Nevertheless, sorption isotherm data on molecular sieve material in the sub 77 K range are rarely found [56–60]. Some results on cryosorption pumping by means of zeolites are reported in Refs. [61–65]. Good cryopumping results for helium have been reported for a LHe-cooled cryopump with a molecular sieve coated cryopanel [66, 67]. However, for the application in cryopumping, the main disadvantage of molecular sieve materials is the hydrophilic character of polar sieves, necessitating high regeneration temperatures [68–70]. In the literature, a significant diffusion-rate limitation has been described for pumping of hydrogen isotopes and helium at molecular sieves, resulting in unstable pumping speed at high flow rates. Correspondingly poor results for co-pumping of mixtures have been reported [71–74]. This is why the current R&D on cryosorption materials is focused mainly on carbon materials.

3.4.1.2   Cryocondensates

The dynamic and static characteristics of sorption by condensed gases depend on several factors, like the physical properties of the sorbent (interaction potentials), the structure of the frost layer (grain size, number of defects), temperature during layer deposition, and temperature at which the adsorption occurs. These many influences render it more difficult to achieve a reliable pump performance than with other sorbent materials. However, vacuum cryocondensates of gases formed under optimal conditions are not essentially inferior to zeolites or activated charcoals. Typical adsorbate/condensate combinations are He/Ar, He/SF_6 or H_2/CO_2.

There are two different techniques to involve cryocondensates for cryopumping (see Section 3.1), namely the pre-frost and the concurrent method. Both methods have been applied successfully for pumping helium on argon in several large fusion machines. The underlying physics of helium cryosorption on solid argon has therefore been investigated comprehensively [75], as this is the only application which gained practical importance. However, lots of other cryocondensates to pump hydrogens, neon and/or helium were investigated, especially by Yuferov et al. [76–80].

According to the pre-frost technique, the condensate layer is predeposited on a blank cryosurface prior to the actual pumping operation. In this case, the gas being pumped interacts with a static sorbent, which gets saturated layer by layer [81–85]. The condensate layer must be built up in a defined way to have a sufficiently porous structure and is usually about some μm thick. With respect to the pumping mechanism, this is based on standard cryosorption, but the achievable equilibrium pressures are lower than for other sorbent materials.

However, the pumping efficiency achievable for pure gases is often very much decreased when mixtures are pumped due to a blockage of the frost pores by the other gas species. Very important for obtaining a porous structure that can be penetrated by the gas pumped is the temperature of condensation of the adsorbent gas [83, 86]. Each combination of adsorbent and adsorbate has its own optimum condensation temperature, which is between 4 and 10 K for hydrogen or helium as adsorbates. At lower temperatures, the adsorption process is limited to sites near the surface of the condensate layer. Only when the temperature is high enough, can the adsorbate molecules be transferred to sites with more favourable energy levels inside the condensate layer. Thus, the active surface is in the order of some 100 m^2/g. The efficiency of the pumping process is determined by the ratio of the number of molecules of the sorbent gas to the number of molecules of the gas to be pumped, which is necessary to obtain appreciable pumping speeds. This ratio is quite high, for example of the order of 20 Ar atoms to pump one He atom at 4.5 K. Nevertheless, Ar is very much suited as cryosorbent, as it has a very high thermal conductivity and effectively removes the heat released during adsorption of helium.

Alternatively, the adsorbent can be injected continuously with the process gas to be pumped; this is the classical mechanism of how to realise cryotrapping pumping. Ar trapping was comprehensively investigated by Hengevoss and Boissin [87–89]. The latter developed the Ar spray technique with a special gas injection manifold. It is convenient to carry out when a cryocondensation pump is readily available for the vacuum system. The advantage of concurrent injection is the availability of fresh frost throughout the pumping process, whereas in the case of pre-frosting, deleterious effects leading to considerably reduced pumping speeds have been observed, e.g., due to icing of other gases present over the frost surface and thus blocking the pathways into the bulk. For cryotrapping, of H_2 on Ar at 4 K, the ratio of the number of adsorbed particles to the sorbent particles becomes equal to 1 and even higher.

However, the biggest disadvantage of using cryocondensates is the considerable increase in the amount of gas which has to be dealt with during regeneration by correspondingly greater sized forepumps.

3.4.1.3 *Activated charcoal*

Activated charcoal sorbents are complex products, as they are manufactured from a wide variety of natural precursors, such as coconut shell, wood, lignite, bitumen, pitch, or peat. The structure of activated carbon is characterized by amorphous regions embedded in well-ordered graphite-like microcrystalline regions, which are formed by regular hexagonal rings. Two different ways are used to activate the charcoal, i.e., increase porosity thus leading to many functional groups on the surface: chemical activation involves the addition of compounds such as phosphoric acid to the parent feedstock prior to carbonization; physical activation refers to gasification of the carbon (introduction of oxygen). The type of raw material, the specific additives, the carbonization and activation temperatures are of great importance in the preparation of activated carbons with respect to their porous structure. Carbons are usually categorized according to the particle shape and size into powders, granules, and formed material (spheres, pellets or fibres). The suitability of an activated carbon for a particular application depends on the ratio in which pores of different sizes are present. The study of carbon materials and their characterization is a lively scientific field of its own.

The broad benchmark studies for different cryosorption materials (references above) unanimously revealed that activated charcoals, especially coconut-shell-based materials, have optimum pumping characteristics. Consequently, numerous investigations on cryosorption pumping involving charcoal as sorbent have been reported and will be used for comparison in the following sections of this paper (e.g., Refs. [90–96]). Nevertheless, sorption equilibrium data for different cryogenic gases in the sub 77 K range are still scarce [56–58, 97–103]. An additional advantage of charcoal compared to molecular sieves is the moderate temperature of about 400 K required to achieve

complete regeneration, whereas molecular sieves would have to be heated up to 300°C for reactivation. This high temperature is incompatible with the use of vacuum seals and gaskets. Carbon has a greater capacity than molecular sieves and is less sensitive to impurity accumulation and water pre-loading.

Thus, we recommend charcoal as the material of choice in operating with the large flow rates and impure gases encountered.

For application as sorbent for cryopanels, the sorbent has to be bonded to a surface. In order to develop the optimum panel set-up, material aspects (sorption isotherms, pore distribution) have to be combined with application aspects (compatibility with bonding agent, thermal cycling, bonding technique). A special bonding technique developed at Forschungszentrum Karlsruhe has been benchmarked within comprehensive thermal cycling tests and no deterioration or thermal degradation has been detected [55]. Some sample panels were manufactured, and the pumping speed for helium was measured. The results are shown in Fig. 8 which illustrates the different significance of the capacity of charcoal when related to unit mass or to the available panel surface. Thus, the material yielding the lowest mass specific capacity for He provides the highest gas loads, when related to the panel surface. This is due to the fact that the available capacity for the cryopanel is not limited by the sorption performance itself, but by the coating process, yielding thin layers for powders and thick layers for charcoal granules.
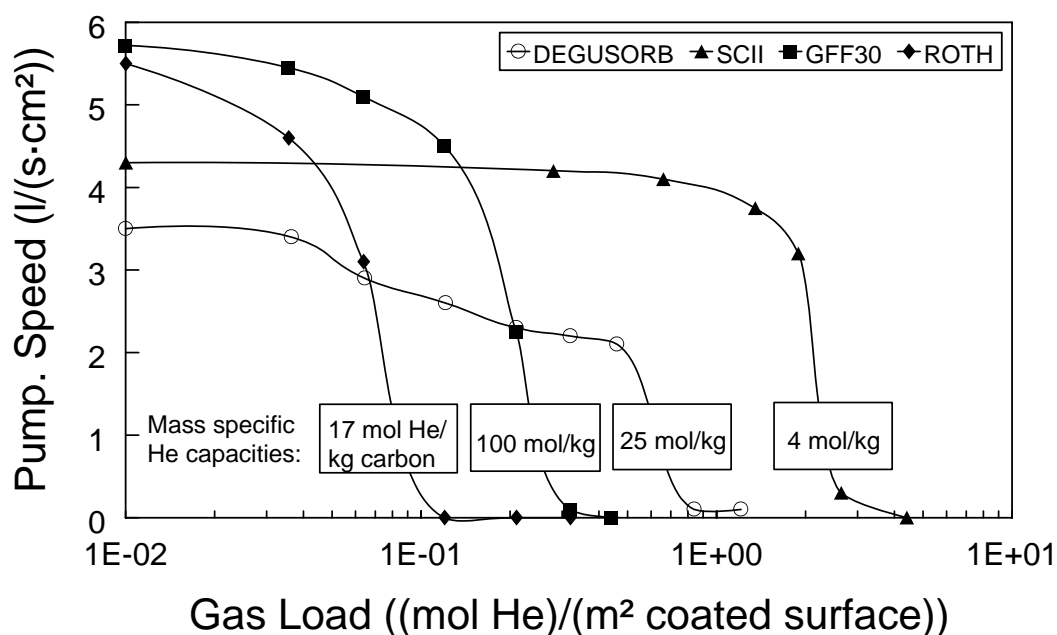

Fig. 8: Pumping speed values for helium at 5 K with different activated charcoal materials, plotted in surface-related coordinates. The materials are pellets (DEGUSORB, 1.5 mm diameter, 5 mm long), granules (SCII), and powders (GFF30, ROTH). DEGUSORB is very close to the materials used in commercial cryopumps.

At Forschungszentrum Karlsruhe, a stage-wise programme was performed in the 1990s to identify the 'best' activated charcoal + bonding technique for nuclear fusion applications (concurrent pumping of helium and hydrogen isotopes at high throughputs). Recently, the class of novel super-high surface area carbon fibre materials (above 2000 m^2/g) has been included. Finally the SCII material (Fig. 8) has become the reference cryosorbent. It is a coconut-shell-derived, granular (US mesh size 12 × 30), microporous (peak at ~ 0.8 to 0.9 nm) activated charcoal material. The reference coating leads to a surface related carbon coverage of ~ 450 g/m^2.

The test programme also showed that the charcoal with the largest surface area was not that which yielded the best performance data. This is in excellent agreement with what has been reported by Sedgley *et al*. [43]. Consequently, all the tests described in the following parts of this report were performed with this kind of carbon material, unless indicated otherwise. Figure 9 presents photographs of the SCII carbon material, taken at different microscopic scales.
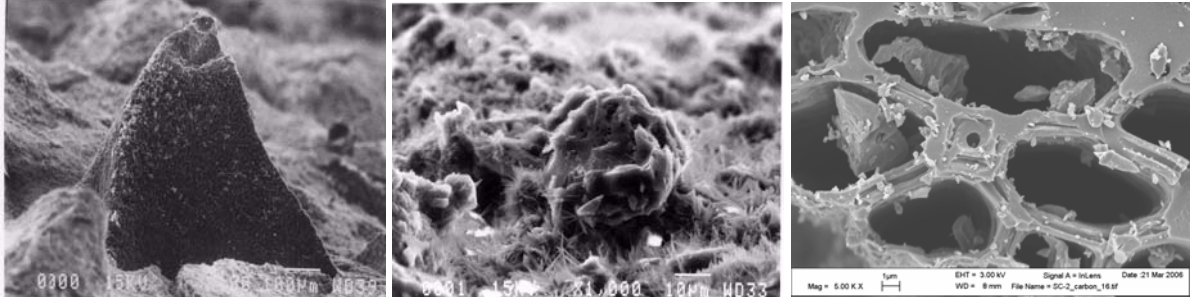

Fig. 9: SEM photographs of the SCII material (100 μm, 10 μm, 1μm scale)

3.4.2 *Standardized criteria for refrigerator-cooled cryopumps*

There is a set of parameters to quantitatively characterize the performance of cryopumps and, thus, the characteristics of the sorbent material therein, see also Table 2. They are listed and discussed in the following section. For refrigerator-cooled cryopumps, which are the only class of cryopumps with large-scale industrial application, the practices of their measurement are fixed by recommendations of the American Vacuum Society (AVS) [104].

1. *Pumping speed*.

The pumping speed is the central scaling criterion for a cryopump and defined as the quotient of the throughput Q of a gas and the working pressure p.

$$S = \frac{Q}{p} . \tag{8}$$

This equation holds, as long as the ultimate pressure of the pump is negligible against the working pressure, which is usually the case. It is equivalent to a volume rate of flow and is expressed in l/s, referenced to $T^* = 273.15$ K. To convert to number of particle or amount of substance based units, the ideal gas law can be used:

$$p \cdot V = n \cdot R_0 \cdot T^* , \tag{9}$$

where V denotes the volume of the vacuum chamber, n the number of moles of gas present, and R_0 the universal gas constant $R_0 = 8.3145$ J/(mol·K).

For easy intercomparison of different pumps, the pumping speed is often related to a typical area, such as the cryopanel area or the entrance cross-section.

2. *Maximum throughput*.

This is the maximum constant gas flow rate which can be pumped by a cryopump at temperatures below 20 K in the second stage. The throughput is usually expressed in (Pa·m^3)/s, taken at T^*.

3. *Pumping capacity*.

The pumping speed decreases with an increasing amount of pumped gas. For adsorbed gases in particular, the pumping speed asymptotically reaches zero. To have a comparable and reproducible measure, the pumping capacity is defined as the quantity of gas that has been pumped until pumping

speed has been reduced to 50% of the initial value. The test for determining the capacity must be run at constant throughput, so that a decrease of 50% in pumping speed is indicated by a corresponding increase of 100% in pressure. The capacity is expressed in (Pa·m^3).

4. Ultimate pressure.

This denotes the minimum achievable base pressure of a cryopump which has been preconditioned (typically minimum 6 h vacuum bake-out), and which is thereafter operated at minimum temperature for at least 24 h.

5. Cool-down time.

This denotes the elapsed time between turning on the refrigerator of a cryopump at room temperature and achieving temperatures of 100 K in the first stage and 20 K in the second stage.

6. Crossover.

The crossover is defined by the maximum amount of nitrogen gas that can be admitted into the pump in a time interval of 3 s, while the second stage remains at temperatures below 20 K. However, this temperature level has been chosen quite arbitrarily from a physical point of view.

To design a vacuum system properly it must be emphasized that the different properties listed above are strongly interrelated among themselves and must in any case be coupled with the performance characteristics of the backing pump. To prevent overloading during and immediately after switching from pre-evacuation to high vacuum pumping, the crossover must be performed when the gas mass flow from the vacuum chamber is less than the maximum throughput of the cryopump. Moreover, the maximum throughput for the crossover condition must be correlated to the period of regeneration.

3.4.3 Regeneration and safety aspects

Cryopumps retain pumped gases as long as their capacity is not exceeded and the arrays are maintained at appropriate temperature. This condition may arise when the cryodeposit condensed at the baffle blocks the louver aperture or when the surface temperature of the panels covered with frozen gas becomes too high due to the temperature gradient through it. However, the cryopump must be regenerated at the latest when the capacity limit has been reached. The capacity is very large for cryocondensation pumps (only limited by the temperature gradient within thick condensate layers) and smaller for cryosorption pumps (limited by full coverage of the active sorption sites, which may be partly clogged). The correct choice of the sorbent is therefore a vital point in cryopump design.

Regeneration is regularly done by heating the cryosurfaces up so that the captured gas deposits are released. As a result, the pressure in the pump increases strongly so that the gas can be pumped away by mechanical forepumps. Before heating, the isolation valve (most appropriate are gate valves which provide full opening) between the pump and system is closed. As the pumping speed starts to decrease before the maximum saturation capacity is reached, a certain safety margin with respect to the maximum operating time must be ensured. After pumping out the release gas, the pump is cooled down again and, thus, the cryopump is ready to be used for the next pumping period. The isolation valve to the vacuum system must remain closed during cool-down, because contaminants resident in the system might be pumped by the second-stage sorbent material, which may result in the plugging of this material. Thus, a regeneration cycle combines five basic steps:

– Closing of the valve to the system.

– Heating of the panel.

– Pumping down of the released gas.

    – Cool-down of the panel.

    – Opening of the isolation valve.

If the regeneration times needed cannot be complied with by the process (e.g., in high-throughput fusion plasma processes), a quasi-continuous pumping system can be achieved by combination of several cryopumps operated staggered by a certain time interval.

Different methods have been used to achieve the heating of the cryosurfaces [105]. Often, the regeneration comprises partial stages at intermediate temperatures sufficient to release low molecular gases and total stages, which are more time consuming, to release all remaining gases. The regeneration process can also be separated geometrically, e.g., in the case of three-stage pumps (cf. Fig. 5), by confining the heating to parts of the pump. Thus, very efficient fractionation of the different gases can be achieved by intelligent control of the regeneration process. The simplest regeneration method is the natural warm-up. The refrigeration is switched off and the warm-up of the panels occurs by thermal radiation from the environment. After reaching the equilibrium temperature of phase transition or desorption, the captured gas is liberated and the pressure rises. Then, heat transfer via convection and gas conduction starts and leads to a faster warm-up. In most commercial cryopumps, this principle is supported by injection of inert purge gas to accelerate the natural heating by initiation of gas heat conduction. This combined regeneration technique can be performed in a fully automated mode controlled by means of an electromagnetic purge valve and cryogenic temperature sensors fastened to the cryosurfaces. However, it results in increased roughing pump requirements to cope with the increased gas amounts. Therefore, electric regeneration systems based on resistance heaters are offered. Normal regeneration times are of the magnitude of some tens of minutes.

In some cases, the point when regeneration is initiated is not given by capacity and speed aspects, but by safety considerations. For example, when hydrogens are pumped at high throughputs, formation of explosive gas mixture compositions must be avoided in case of a sudden air in-rush due to a leak when the complete pumped gas load has just been liberated [106]. In this case the minimum pressure limit for combustibility may be exceeded. The hydrogen inventory is directly proportional to the period between successive cryopump regenerations, which indicates a need to have a greater number of pumps and to regenerate them at shorter intervals and more rapidly (of the order of some minutes). For these applications, faster heating techniques have been developed, including infrared, glow discharge, microwave and synchrotron radiation (photodesorption) heating. Certain precautions must also be taken, since the cryopumped gases may be released species by species according to their desorption/sublimation curves, rather than mixed.

3.5 Cryopump design

The vacuum technological design of a cryopump aims to maximize the pumping speed S within the existing cooling supply conditions and space limitations. The basic design Eq. (10) shows that apart from the usual parameters such as temperature T, inlet cross section A, and the properties of the gas being pumped (mass M and gas constant R_0), the only parameter left to adjust during design is the capture coefficient c, to which the pumping speed directly scales. The capture coefficient is given by the ratio of the actual pumping speed of the cryopump to the theoretical black hole pumping speed S_{id} and indicates the efficiency of the pump:

$$S = c \cdot S_{id} = c \cdot A_{inlet} \cdot \sqrt{\frac{R_0 \cdot T}{2\pi \cdot M}} \; . \tag{10}$$

Thus, the pumping speed of a cryopump is a function of the geometry of its internal structures, the molecular weight M of the gas being pumped, and temperature. However, as outlined above, a

reference temperature of $T = T^* = 273.15$ K is usually chosen. It should also be noted that it is not correct to compare the pumping speed without referring to the gas. So, a pump with the same pumping efficiency differs, for example, by factor 2.6 in pumping speed between He and N_2, with the lighter gas He having the higher speed.

The ideal speed is reduced, firstly on the path of a particle to the cryosurface due to the limited transmission probability w of the installed baffles etc., and, secondly, by the incomplete adhesion on the cryosurface due to the different types of gas–surface interaction. The latter effects are summarized by an overall sticking probability α (the number of particles sticking to the cryosurface related to the number of particles impinging on it) characterizing the overall gas–surface interaction. By this phenomenological approach, the first-order influences of geometry (summarized by w) are separated from the second-order influences of gas–surface interaction (summarized by α). For the simplified case of parallel arrangements of the panel and the baffle, as typical for commercial refrigerator cryopumps, we have the following simple expression:

$$\frac{1}{c} = \frac{1}{\alpha} + \frac{1}{w} - 1 . \tag{11}$$

Because of this geometry influence, it is not easy to scale the pumping speed from one geometry to another.
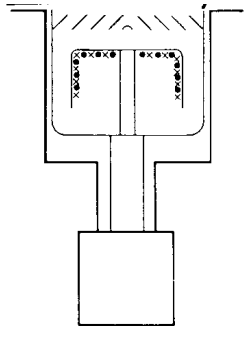
Values for the transmission probability can be derived from compilation textbooks (see the bibliography at the end of this report). The sticking probability itself is determined by many parameters, with temperature, type of gas, and, for adsorption pumping, sorbent pore size distribution and pumped gas amount being the main influential factors. Because of these many influences and because the data retrievable from the literature are scarce and inconsistent, a parametric characterization has been performed for the ITER type charcoal under ITER-relevant conditions, the results of which are summarized in Table 3. As expected, the sticking probability of He, which is the most difficult gas to pump, is a strong function of temperature, whereas the temperature dependence for H_2 is less pronounced. The sticking probability for particles pumped by re-sublimation is higher (up to unity) and less dependent on temperature.

Table 3: Comparison of initial (zero gas load) sticking probabilities for nuclear fusion relevant gases at different temperatures

Temperature (K)	He	H_2	D_2	T_2
5	0.35 [107] 0.25 [108]	0.6 [107]	0.9 [107]	1.0 [109]
7	0.17 [107, 110]	0.5 [111]	–	1.0 [109]
12	0.03 [107]	0.3 [112]	0.85 [112]	–

As an example, based on Eq. (11), Table 4 gives some numerical values for a typical commercial refrigerator cryopump, assuming a transmission probability for the inlet baffle of 0.4, which is typical for a louver. It becomes obvious that the capture coefficient depends strongly on the type of gas being pumped. There results more than an order of magnitude between the gas being pumped best and worst.

Table 4: Characteristic parameters for a standard refrigerator cryopump (first stage at 70 K, second stage at 10 K)

Gas	W	α	C	Where and how pumped	Reference set-up
H_2O	1.0	1.0	1.0	At the inlet baffle by condensation	
T_2, N_2	0.4	1.0	0.4	At the cryopanel front side by re-sublimation	
H_2	0.25	0.6	0.21	At the cryopanel back side by cryosorption	
He	0.25	0.05	0.04	At the cryopanel back side by cryosorption	

One of the advantages of cryopumps is that they can be designed as *in situ* pumps tailor-made according to the available space, dedicated to the specific application. The arrangement of cryopanels and shields is then rather complex so that the application of the simplified Eq. (1) to estimate the capture coefficient is no longer justified. In this case, Monte Carlo simulations of the pump interior have to be performed to calculate the capture coefficient. The pump designer, who has to decide upon the arrangement of the individual pump components, can use Monte Carlo simulations as a study tool. As a design goal, one should aim to come as close as possible to the ideal capture coefficient curve shown in Fig. 10. A pump exhibiting such a performance curve, i.e., with constant capture coefficient over a wide range of sticking probability, would pump practically all gas species at the same pumping speed.
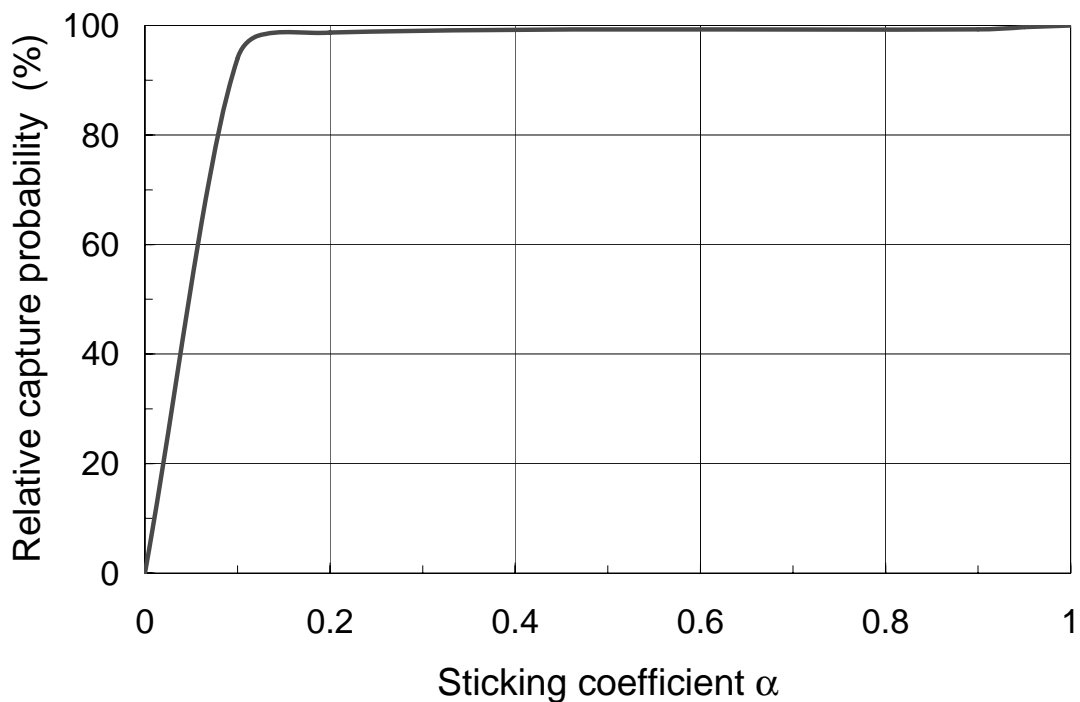

Fig. 10: The 'ideal' curve of the capture coefficient, related to its maximum value at a sticking probability of unity

3.6 Summary of advantages of cryopumping

The practical design of a cryosorption pump is a compromise between several parameters, some of which are mutually contradictory. It is, therefore, evident that to arrive at an optimum configuration is not an easy matter and the final design is possibly best achieved by a combination of theory and experiment. Having reviewed the advantages and limitations of cryosorption pumping, the following list summarizes briefly the advantages.

1. Cryopumping offers unparallelled performance where absolute cleanliness and oil-free conditions are required. Consequently, it is used as a reference for benchmarking contamination introduced from the process side or from other vacuum pumps.

2. Cryopumping is the method of choice for reproducible pumping of water vapour or very humid gas mixtures, as it provides black hole pumping speed (capture coefficient of unity).

3. Cryopumping provides increasing pumping speed with lighter gases.

4. Cryopumping is the most economic solution if highest pumping speeds are required: up to 60 m^3/s (nitrogen) via DN1200 for the biggest commercial pumps. Customized cryopumps can provide biggest pumping speeds via smallest cross-sections (e.g., 100 m^3/s via DN750).

5. Cryopumping based on liquid cryogens does not involve any electric supply (i.e., inherent safety against power breakdowns, full compatibility with applications in magnetic fields) and is totally free of vibration.

6. No mechanically moving parts are present in the vacuum chamber (i.e., highest reliability, minimal maintenance, no bearing and shaft seal problems, no problems with dust contamination, highest safety level).

7. The free orientation of the cryopump allows for installation at places with limited access.

8. Cryopumping provides the possibility of selective pumping.

Besides the conventional refrigerator-cooled cryopumps, cryopumping is mainly used for large-scale R&D applications, such as space simulation [113], plasma physics and thermonuclear fusion [111, 114, 115], particle beam and accelerator systems [116–119]. These pumps are almost exclusively prototypes and dedicated developments.

4 Special regeneration aspects of a cryosorption pump

The operation of a cryosorption pump includes some specialities due to the gas–sorbent interaction, some of which will be discussed in the following sections. A major aspect is the cryopumping mechanism. The fact that a sorbent is present in the pump does not necessarily mean that all gases are really being pumped by adsorption. There are cases where gas is being pumped by condensation on top of the charcoal. In these cases, the charcoal pores may be clogged and the pumping speed for gases being pumped by sorption only may be drastically reduced. Moreover, if it comes to regeneration, the behaviour for all gases is given by the charcoal inside the pump.

Figure 11 shows the result of a defined regeneration test under a constant heating rate with active forepumping. As a result, typical pressure peaks are obtained which indicate gas releases.
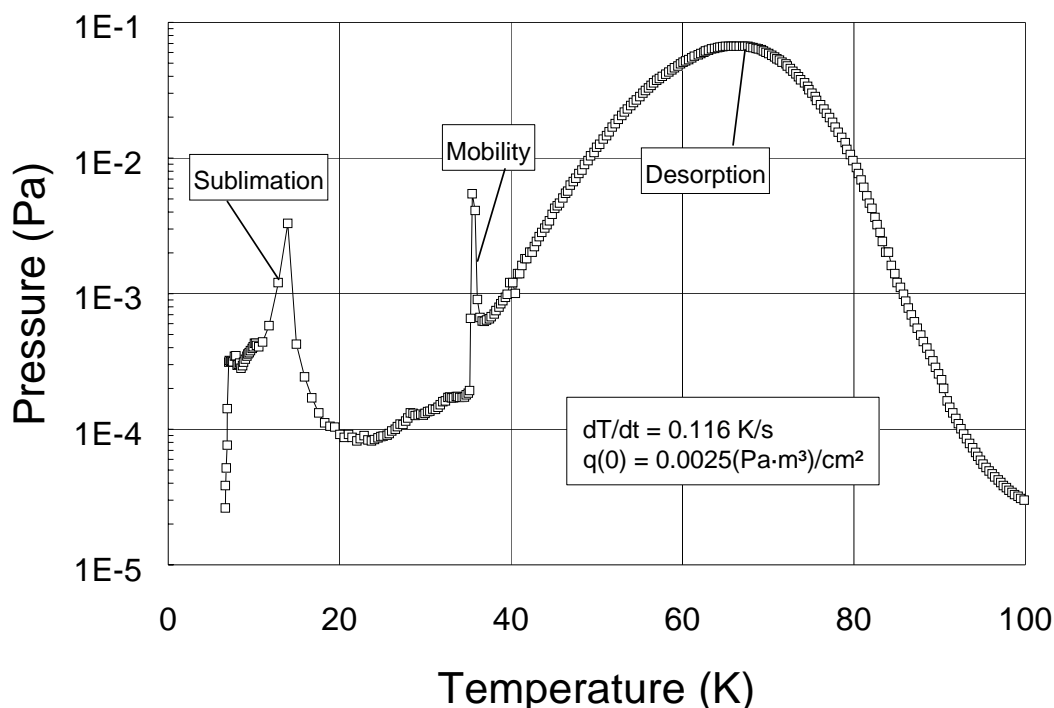
Fig. 11: A temperature programmed desorption experiment for D_2, illustrating mobility effects

The curve in Fig. 11 exhibits three clearly distinguishable peaks. The largest peak in the higher temperature range indicates desorption. The low temperature peak for deuterium can be attributed to the sublimation pressure curve. However, there is a further peak at the intermediate temperature. This peak is a kinetic effect due to dynamic loading, which was described first by Lessard [90], typical for quantum gases. The quantum delocalization of surface molecules follows a strong, exponential functional relation between the residence time of a molecule impinging and the sorbent temperature. At a certain threshold temperature, the surface mobility of the adhered molecules is high enough so that they can clear the surface. In this activated state, the molecules can migrate deeper into the sorbent pores, but are at the same time liberated more easily. Consequently, a pressure peak can be observed. This boundary temperature also depends on the gas load situation (intermittent or continuous throughput) [91] and can be exploited to increase the loading capacity of the sorbent by heating beyond this temperature limit, which helps the molecules to disperse rapidly into the sorbent bulk, and thus, offers new active surface sites for cryopumping. In this respect, the static sorbent capacity, which is known to increase with decreasing temperature, is not necessarily the correct measure to judge a real dynamic cryopumping process. To evaluate the holding time of a cryopump, capacity aspects and mobility aspects have to be combined.

Figure 12 is another temperature programmed desorption experiment to illustrate the fractionation of the gases pumped during controlled heating. The first peak is formed by helium desorption and partial release (to a small extent) of deuterium due to mobility and sublimation. The second peak is produced by desorption of the remaining deuterium. Thus, a fine separation between the two species can be achieved by heating to an intermediate temperature range of about 30 K. Alternatively, the sorbent can be used for selective pumping, if operated at this temperature, i.e., only the hydrogens will be pumped, whereas helium will not. This application is of vital interest for trace analysis and leak detection devices for large vacuum systems [120].
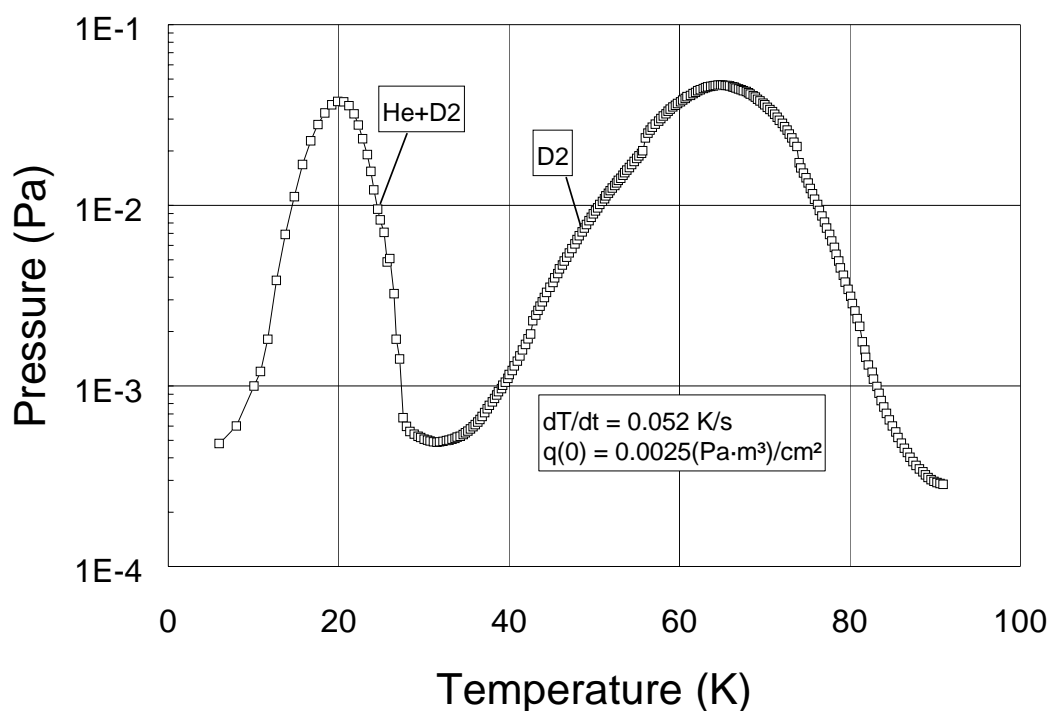
Fig. 12: A temperature programmed desorption experiment of a mixture with 10% helium in deuterium, illustrating fractionation effects

As illustrated in Fig. 13 (and Table 3), helium, which is the gas that is most difficult to pump, and has by far the lowest sticking probabilities, is also the most sensitive to temperature increase. The strongest helium release will take place in the temperature range between 10 and 20 K. Figure 13 illustrates the 3D relationship between pumping speed, temperature, and capacity limit for helium. The capacity is given related to the coated surface (at 450 g charcoal/m^2).
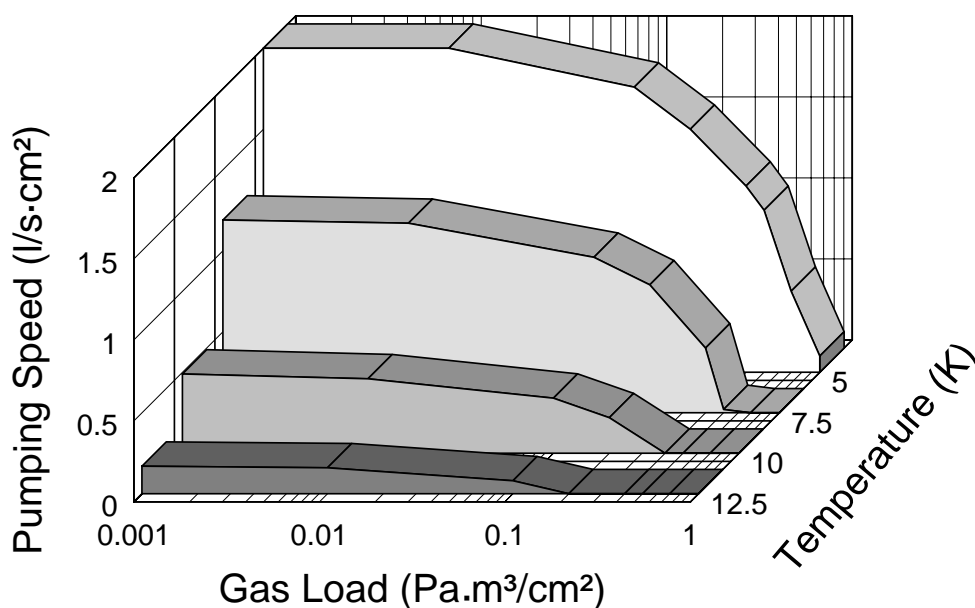
Fig. 13: Performance map of helium croyosorption on activated charcoal

Hydrogen H_2 also shows some sorption capacity limitation, but this is at least a magnitude higher.

As outlined above, species being pumped by sorption and species being pumped by condensation are pumped on different surfaces. The latter are cryocondensed at the 80 K baffle arrays and, in this respect, will not immediately influence the sorption performance of the panels downstream. However, if regenerated, the condensed species will evaporate as soon as the temperature becomes equivalent to the boiling temperature at the corresponding partial pressure and may re-adsorb on the charcoal, as the temperatures sufficient to sublimate the cryodeposits are still sufficient to provide for a sorption at the charcoal. By this mechanism, all gas species, no matter where pumped at first, will have a principal impact on the sorption panels. An example of this effect is illustrated in Fig. 14, which shows the interaction of sublimation from the heated baffle stage and subsequent adsorption at the sorption stage.
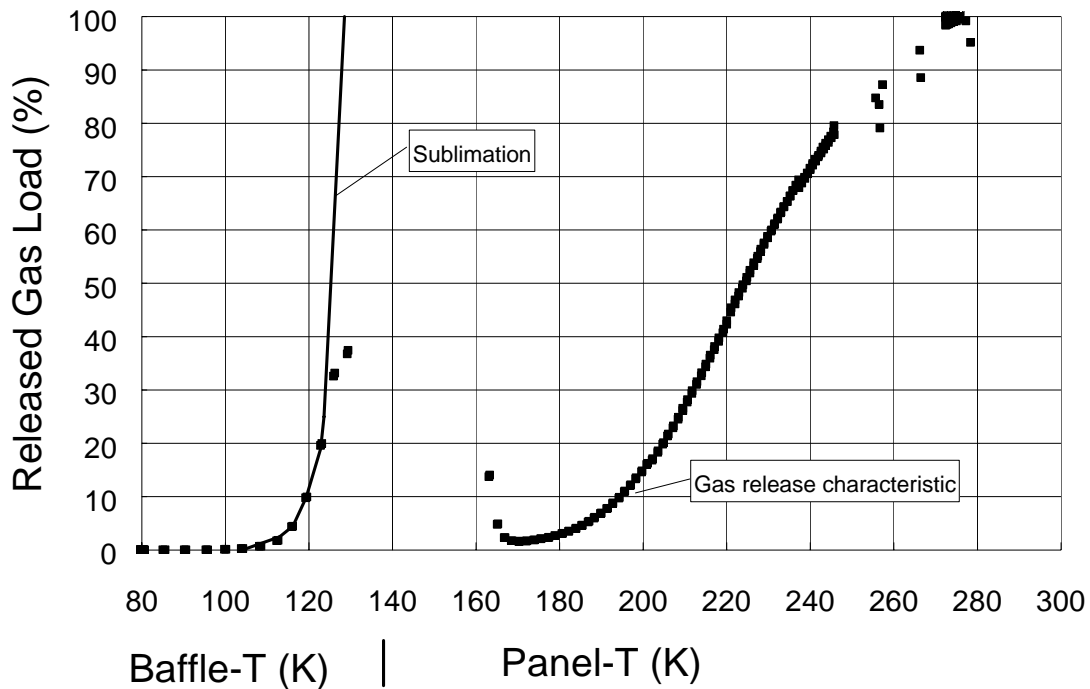

Fig. 14: Interrelation of sublimation of the condensed CO_2 pumped at the baffle and re-adsorption on the charcoal coated panel

This measurement was performed during regeneration by heating up the panel directly and, via radiation and starting gas heat conduction, the baffle indirectly. Therefore, there is a certain driving temperature difference between panel and baffle. Nevertheless, the molecules released from the baffle, will instantaneously stick to the panel, even at the higher temperature there. Hence, the performance of each cryopump with a sorption stage is governed by the ad-/desorption process, even for those gases which at first are not pumped by cryosorption, but condensed at the baffle. This has major implications on cryopump operation, because there will often be a pumping situation involving a cryosorbent which is pre-loaded with a certain amount of condensables. Figure 15 gives typical desorption temperature curves needed to achieve efficient regeneration of the charcoal. Of course, desorption from a sorbent can also be stimulated by pressure reduction. However, this is a much slower process and is therefore only used to increase sorption efficiency in parallel to the usual temperature increase.
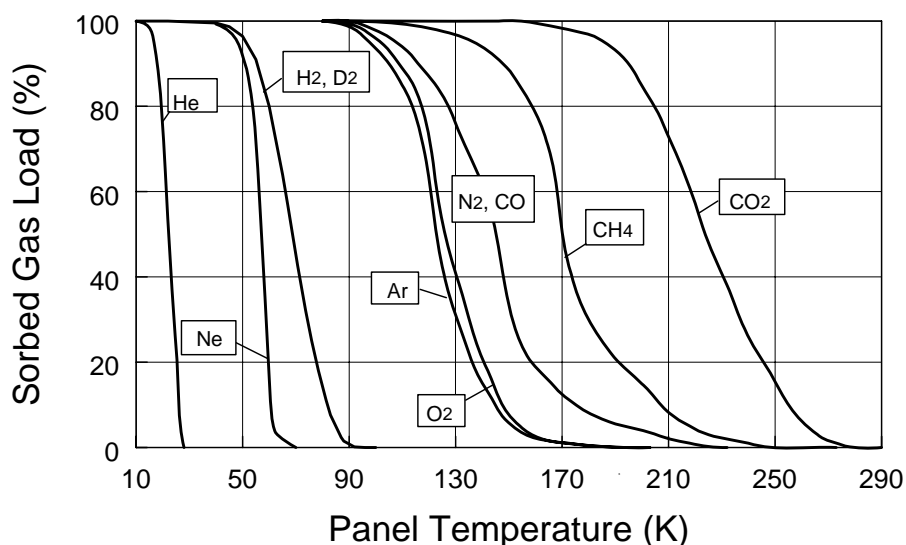
Fig. 15: Temperature-induced desorption curves

This leads to the detailed investigation of the dynamics involved in the sorption pumping process, which is characterized by limitations due to saturation and poisoning. The saturation limit is reached when the maximum gas load has been pumped. The reduction of pumping speed due to accumulation of trace components in the gas mixture to be pumped, which are not being released during normal regeneration procedures, is another important feature of cryopump operation [120].

5 Application examples

This section features two selected application examples for customized cryopumps.

5.1 Combined refrigerator/liquid cryogen pump

Figure 16 shows a three-stage cryopump which was developed for space simulation chambers. These applications usually require a vacuum in the order of about 10^{-4} Pa. The inlet baffle is cooled with liquid nitrogen to 77 K. Inside the pump, there is a two-stage GM cooler, featuring a 50 K condensation stage and a 20 K low temperature sorption stage (charcoal covered). The regeneration can be done via electrical heaters attached to the cryosurfaces, or with warm gas purging, alternatively. The pump features an opening diameter of 1.25 m and has a nominal pumping speed of 50 m^3/s for nitrogen (capture coefficient $c = 0.35$) and hydrogen (capture coefficient $c = 0.09$).

Fig. 16: Large cryopump for space simulation chambers

5.2 ITER cryopumps

ITER is the next generation thermonuclear fusion device of the tokamak type, and represents the experimental step between today's studies of plasma physics and tomorrow's electricity-producing fusion power plants. It is based on a deuterium–tritium plasma operating at over 100 million K, and will produce 500 MW of fusion power. Control of the gas throughput, especially the helium ash produced by D–T fusion reactions, is one of the key issues affecting the performance and achievable burn time of a fusion reactor.

The ITER machine includes three large cryogenic high-vacuum pumping systems. One is for evacuation and maintenance of the required pressure levels in the torus (1350 m^3); the second is for generation of the required vacuum conditions in the neutral beam injectors (NBI) (570 m^3), which are used to heat up the plasma by injection of highly energetic accelerated neutral H and D particles; and the third is for provision of the insulation vacuum in the cryostat (8400 m^3), which houses the superconducting coil system. The typical pressures inside the torus and the NBI systems are in the range of 1 to 10 Pa. Thus, the rationale to use cryogenic pumping is not given by the need to establish low pressures, but by the need to process very high gas throughputs necessitating highest pumping speeds. As ITER will be a burning deuterium–tritium plasma experiment, the vacuum system must not only be designed for the high magnetic and electric fields but also withstand disruption events creating high mechanical loads, radiation, and be compatible with tritium. The latter excludes the use of any organic material in direct or sealing contact with the process gas. These requirements can be met best with cryogenic pumps without any moving parts, backed by a multi-stage forepump train based on roots pumps.

All large high-vacuum pumping systems on ITER are based on charcoal-coated cryopanels forced-cooled by 4.5 K supercritical helium at 0.4 MPa. Extensive preparatory tests were run in the past to find an optimum combination of sorbent type and bonding cement, resulting in a ~ 1 mm thick layer of specific granular activated charcoal, bonded by an inorganic tritium-compatible cement. The ITER type charcoal is a microporous, granular, highly activated carbon, derived from coconut shells. An automatic coating facility using a special spray technique has been developed at Forschungszentrum Karlsruhe. Figure 17 shows a photo of the typical coated cryopanels which are used as modules to build up the sorption cryosurface in any required geometry.
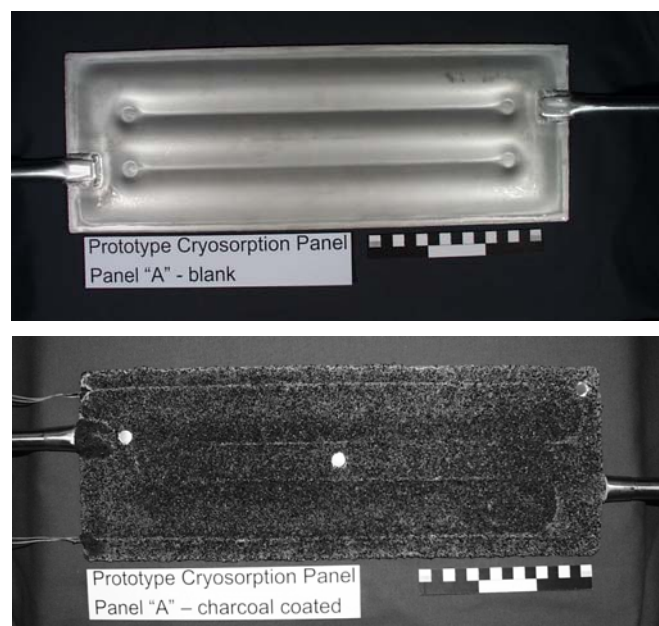

Fig. 17: Photographs of a prototype cryosorption panel (150 mm wide, 450 mm long); in blank state (top) and ready coated (bottom, here also equipped with heaters and prepared spots for temperature sensors)

Although being tailor-made pumps, the cryopumps share the same basic features as every cryopump, namely a low-temperature circuit (the 4.5 K cryosorption panel system) and an intermediate temperature circuit (the 80 K thermal shielding and inlet baffle system) to reduce thermal loads on the low-temperature circuit. The temperatures are given by the available cooling conditions at ITER. The system of the eight ITER torus cryopumps is the most complex on ITER. A speciality of the ITER cryopumps is the inclusion of an inlet valve, to control the throughput and to isolate the pump from the torus during regeneration. The inlet valve adds an additional degree of freedom to the pump control. Figure 18 illustrates the principle circular design of the ITER torus cryopumps, featuring 28 cryosorption panels [121]. Figure 19 shows two photographs of a half-scale model pump version which was manufactured some years ago. The pumping speed results of the model pump performance are summarized in Fig. 20.
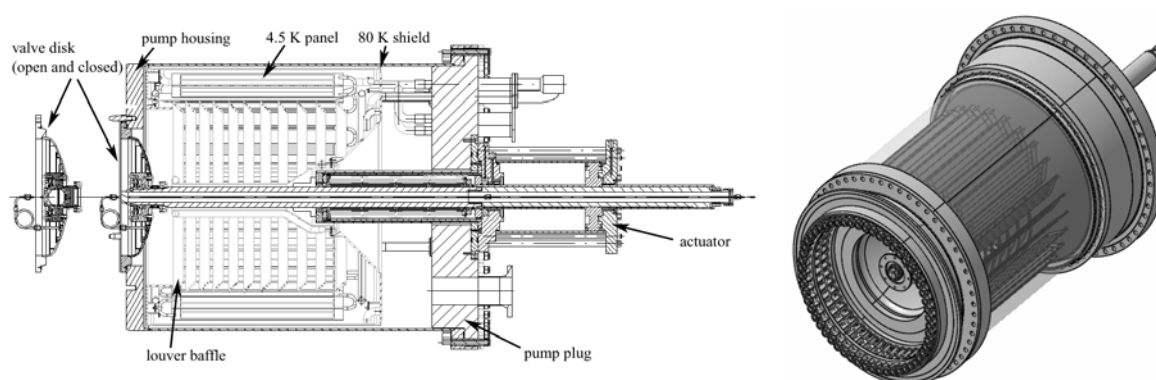

Fig. 18: Design of the ITER torus cryopump (nominal free molecular pumping speed of 50 m^3/s, DN 800). 2D cut (left) and a 3D view (right, without outer 80 K shield and housing)
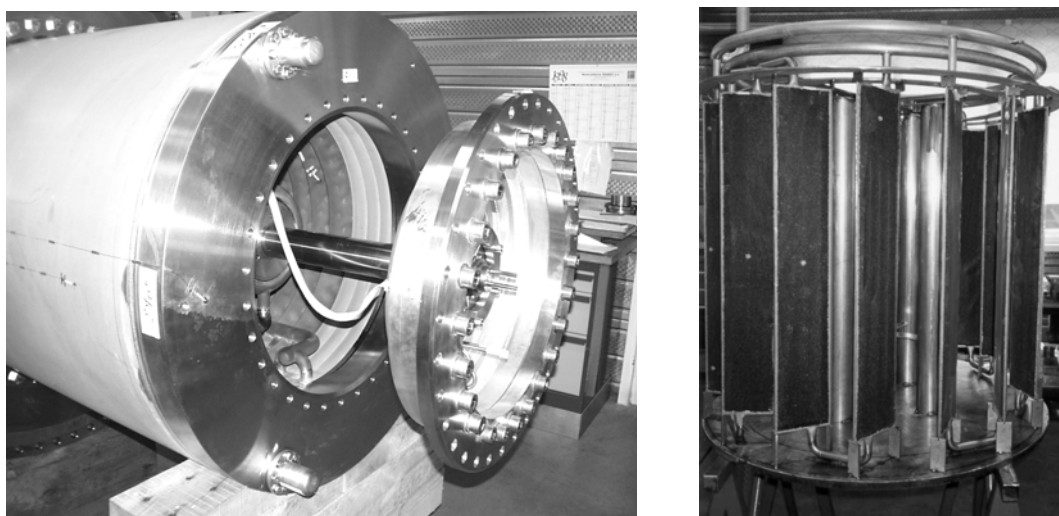

Fig. 19: Photos of the model pump, showing the opened inlet valve (left) and the interior cryopanel circuit (right)

Figure 20 illustrates the valve control effect. The pump performance under high throughput conditions is a good fingerprint of the robustness of the pump design, as this involves maximum heat loads on the cryopanel system. The measured pumping speed values are plotted twice, on the left-hand side as a function of the pressure inside the pump, on the right-hand side as a function of the pressure at the pump inlet. The difference of the 100% curves indicates the pressure loss of the fully opened valve, which is about 1 decade over the whole range of investigated flowrates. The vertical interconnecting lines combine points of the same throughput. For increasing flowrate, the pressure is

also increased. However, the pressure situation inside the pump depends only on the throughput and is completely decoupled from the valve position. Whereas the pressure at the pump inlet, which is the decisive one since it is closely linked to the torus pressure, can be controlled by appropriate adjustment of the valve position. Thus, the valve is a helpful tool to make the pump more flexible and suited to establish the specified inlet pressure range.
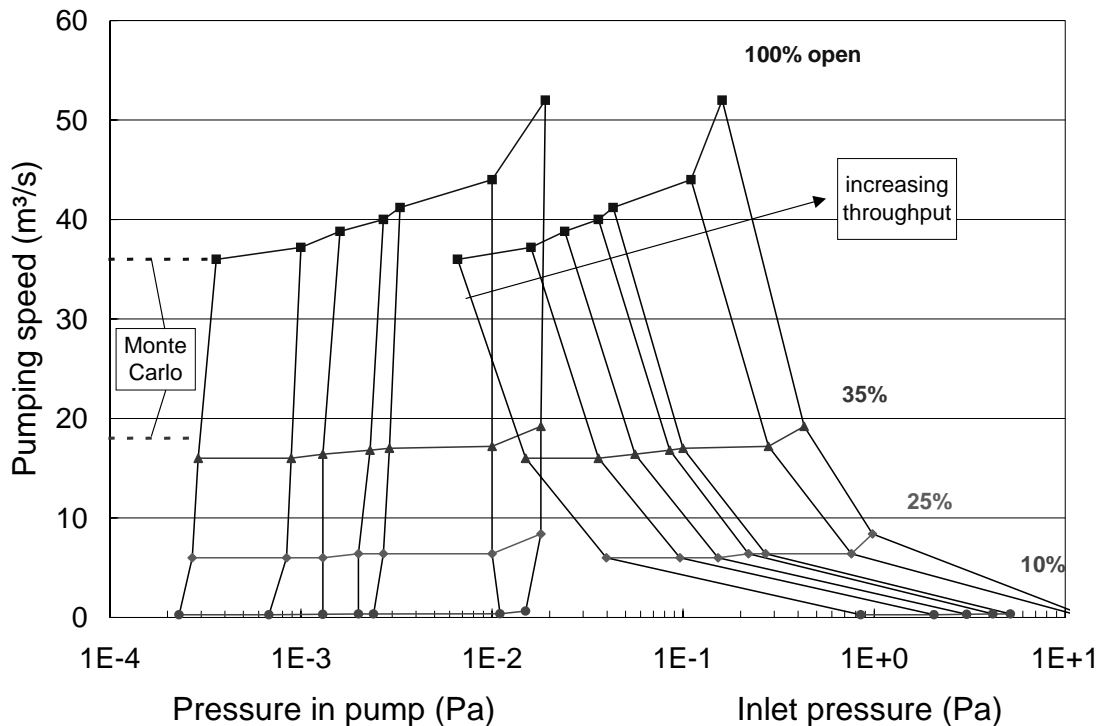

Fig. 20: Pumping characteristics of the model pump. Results for a typical fusion exhaust model gas, consisting of 87% D_2, 10% He, and 3% impurities (CO, CH_4, CO_2, O_2). The throughput was varied [between $6 \cdot \times 10^{-6}$ Pa $\cdot$ m^3/(s $\cdot$ cm^2) and 4×10^{-4} Pa $\cdot$ m^3/(s $\cdot$ cm^2)] at constant valve position (100%, 35%, 25% and 10% open).

The increase of pumping speed with increasing throughput indicates that the pump will be under transitional flow regime inside the pump during regular operation.

The same design principles, but without an inlet valve, will be applied to develop the NBI cryopumps. The required integral pumping speeds are 3800 m^3/s for H_2, and 2600 m^3/s for D_2, respectively [122].

6   Conclusions and prospects

This review articles gives an introduction to the underlying basics and different aspects of practical cryopumping, and reviews the state of the art. The modelling of tailor-made cryopumping is a demanding field because it cross-links many different disciplines such as vacuum science, cryogenic engineering, surface and physical chemistry. It further brings together in a unique way technological and physics aspects. In view of the large R&D projects coming up in the next few years, further development work and fundamental investigation of cryopumps will be necessary. This is the main guideline for the research to be done in the future.

References

[1] ISO 3529/1–3, *Vacuum Technology: Vocabulary* (International Organization for Standardization, Geneva, Switzerland, 1981).

[2] R.T. Jacobsen, S.G. Penoncello, and E.W. Lemmon, *Thermodynamic Properties of Cryogenic Fluids* (Plenum Press, New York, 1997).

[3] C. Benvenuti, R.S. Calder and G. Passardi, J. Vac. Sci. Technol. **A 13** (1976) 1172.

[4] A.G. Mathewson, Vacuum **44** (1993) 479.

[5] S.G. Sydoriak, T.R. Roberts and R.H. Sherman, J. Natl. Bur. Stand. **68A** (1964) 559.

[6] B. Fellmuth and G. Schuster, Metrologia **29** (1992) 415.

[7] V. Arp, R.D. McCarty and J. Fox, *HEPAK Code* v. 3.40 (Cryodata Inc., Louisville, CO, 1997).

[8] P.C. Souers, *Hydrogen Properties for Fusion Energy* (University of California Press, Berkeley, 1986).

[9] K. Erents and G.M. McCracken, Vacuum **21** (1971) 257.

[10] J.P. Hirth and G.M. Pound, *Condensation and Evaporation* (Pergamon Press, Oxford, 1963).

[11] M.M. Eisenstadt, J. Vac. Sci. Technol. **7** (1970) 479.

[12] V. Ponec, Z. Knor, and S. Černy, *Adsorption on Solids* (Butterworths, London, 1974).

[13] G.C. Maitland, M. Rigby, E.B. Smith and W. Wakeham, *Intermolecular Forces* (Clarendon Press, Oxford, 1981).

[14] A.W. Adamson, *Physical Chemistry of Surfaces*, 5th ed. (John Wiley, New York, 1990).

[15] L.W. Bruch, M.W. Cole and E. Zaremba, *Physical Adsorption: Forces and Phenomena* (Clarendon Press, Oxford, 1997).

[16] M.G. Kaganer, *Thermal Insulation in Cryogenic Engineering* (IPST Press, Jerusalem, 1969).

[17] Chr. Day, B. Kammerer and A. Mack, Adv. Cryog. Eng. **43** (1998) 1327.

[18] J.R. Howell, *A Catalog of Radiation Configuration Factors* (McGraw-Hill, New York, 1982).

[19] R. Siegel and J.R. Howell, *Thermal Radiation Heat Transfer*, 2nd ed. (Hemisphere Publishing, New York, 1981).

[20] J.M. Hammersley and D.C. Handscomb, *Monte Carlo Methods* (Chapman and Hall, London, 1979).

[21] G.L. Saksaganskii, *Molecular Flow in Complex Vacuum Systems* (Gordon and Breach, New York, 1988).

[22] S. Tsujimoto, A. Konishi and T. Kunitomo, Cryogenics **22** (1982) 603.

[23] C. Benvenuti, D. Blechschmidt and G. Passardi, J. Vac. Sci. Technol. **19** (1981) 100.

[24] G.S. Ash, Calculation of pumping speeds of high vacuum systems in molecular flow, *Proc. 37th Annual Technical Conference Society of Vacuum Coaters*, 1994, pp. 100–109.

[25] W. Obert and G. Perinić, Vacuum **43** (1992) 163.

[26] H.O. McMahon and W.E. Gifford, Adv. Cryog. Eng. **5** (1960) 354.

[27] P.D. Bentley, Vacuum **30** (1980) 145.

[28] J. Harvell and P. Lessard, Semiconductor International, June 1991.

[29] B. Engers and H.U. Bauer, Surface and Coatings Technol. **116** (1999) 705.

[30] Y. Shiokawa, T. Kikuchi and M. Ichikawa, Vacuum **47** (1996) 803.

[31] T. Shigi, M. Nakamura, M. Yamaguchi, M. Azuma and M. Yanai, Cryogenics **30** (Supplement) (1990) 523.

[32] J.P. Perin, D. Henry, R. Vallcorba, J.J. Cordier and F. Samaille, Vacuum **48** (1997) 743.

[33] J.L. Hemmerich and E. Küssel, J. Vac. Sci. Technol. **A 8** (1990) 141.

[34] A. Horbowa and P. Dolegieviez, Vacuum system performances on spiral facility, *Proc. 15th Int. Conf. on Cyclotrons and Their Applications*, Caen, France, 1998.

[35] M. Gouge and C. Foster, *Argon Frost Continuous Cryopump for Fusion Application*, Report DOE/ER/81236-6 (Department of Energy, Washington, USA, 1995).

[36] Chr. Day and V. Hauer, Adv. Cryog. Eng. **50** (2004) 75.

[37] D.D. Do, *Adsorption Analysis: Equilibria and Kinetics* (Imperial College Press, London, 1998).

[38] F. Rouquerol, J. Rouquerol and K. Sing, *Adsorption by Powders and Porous Solids* (Academic Press, London, 1999).

[39] S.J. Gregg and K.S.W. Sing, *Adsorption, Surface Area and Porosity*, 2nd ed. (Academic Press, London, 1982).

[40] D. Perinić, H. Haas and A. Mack, Fusion Eng. Design **18** (1991) 79.

[41] D. Perinić, H. Haas and A. Mack, Cryogenics **30** (Supplement) (1990) 509.

[42] D. Perinić, H. Haas and A. Mack, Adv. Cryog. Eng. **39** (1994) 1553.

[43] D.W. Sedgley, G. Tobin, T.H. Batzer and W.R. Call, J. Vac. Sci. Technol. **A 5** (1987) 2572.

[44] D.W. Sedgley, A.G. Tobin, T.H. Batzer and W.R. Call, Nuclear Eng. Design **4** (1987) 149.

[45] D.W. Sedgley, T.H. Batzer and W.R. Call, J. Vac. Sci. Technol. **A 6** (1988) 1209.

[46] A.G. Tobin, D.W. Sedgley, T.H. Batzer and W.R. Call, J. Vac. Sci. Technol. **A 5** (1987) 101.

[47] D.W. Sedgley, Fusion Eng. Design **10** (1989) 217.

[48] L.S. Gurevich, I.N. Moreva, V.V. Petrovsky, A.V. Pustovoit and A.S. Shelukhin, Plasma Devices and Operation **2** (1994) 287.

[49] L.S. Gurevich, V.V. Petrovski and A.V. Pustovoit, Plasma Devices and Operation **1** (1990) 97.

[50] M. Xu and Y. Matsui, J. Vac. Sci. Technol. **A 13** (1995) 132.

[51] J. Ma, D.L. Kingsbury, F.-C. Liu and O.E. Vilches, Phys. Rev. Lett. **61** (1988) 2348.

[52] V.V. Anashin *et al.*, Vacuum **76** (2004) 23.

[53] V.V. Anashin *et al.*, Vacuum **75** (2004) 293.

[54] V.V. Anashin *et al.*, Vacuum **72** (2004) 379.

[55] Chr. Day, H. Haas, N.T. Kazakovsky, A. Mack, D.K. Murdoch, D. Röhrig and G.L. Saksagansky, Summarized results of the cryosorption panel test programme for the ITER cryopumping system, *Proc. 17th IAEA Fusion Energy Conference*, Yokohama, Japan, 1998, vol. 3, pp. 1073–1076.

[56] R. Yanik, U. Yanik and C. Heiden, J. Low Temp. Phys. **45** (1981) 443.

[57] D. Basmadjian, Can. J. Chem. **38** (1960) 141.

[58] D. Basmadjian, Can. J. Chem. **38** (1960) 149.

[59] J.G. Daunt and C.Z. Rosen, J. Low Temp. Phys. **3** (1970) 89.

[60] M. Jäckel and R. Bartel, Exp. Tech. Phys. **28** (1980) 153.

[61] P.J. Gareis and G.F. Hagenbach, Ind. Eng. Chem. **57** (1965) 27.

[62] S.A. Stern, J.T. Mullhaupt, R.A. Hemstreet and F.S. diPaolo, J. Vac. Sci. Technol. **3** (1965) 165.

[63] G.E. Grenier and S.A. Stern, J. Vac. Sci. Technol. **3** (1966) 334.

[64] S.A. Stern, R.A. Hemstreet and D.M. Ruttenber, J. Vac. Sci. Technol. **3** (1966) 99.

[65] L.C. Pittenger, Adv. Cryog. Eng. **23** (1978) 648.

[66] R.J. Powers and R.M. Chambers, J. Vac. Sci. Technol. **8** (1971) 319.

[67] H.J. Halama and J.R. Aggus, J. Vac. Sci. Technol. **11** (1974) 333.

[68] D. Cheng and J.P. Simson, Adv. Cryog. Eng. **10** (1965) 292.

[69] S.A. Stern and F.S. diPaolo, J. Vac. Sci. Technol. **4** (1967) 347.

[70] D. Burghardt, A. Mack, D. Perinić, H. Reichert and D. Röhrig, Vacuum **45** (1994) 547.

[71] H.J. Halama, H.C. Hseuh and T.S. Chou, Adv. Cryog. Eng. **27** (1982) 1125.

[72] H.J. Halama and J.R. Aggus, J. Vac. Sci. Technol. **12** (1975) 532.

[73] P.W. Fisher and J.S. Watson, J. Vac. Sci. Technol. **16** (1979) 75.

[74] C.F. Dillow and J. Palacios, J. Vac. Sci. Technol. **16** (1979) 731.

[75] G.V. Kachalin, A.P. Kryukov and S.B. Nesterov, Low Temp. Phys. **24** (1998) 97.

[76] V.B. Yuferov, Low. Temp. Phys. **19** (1993) 413.

[77] V.B. Yuferov and P.M. Kobzev, Sov. Phys. Tech. Phys. **14** (1969) 427.

[78] V.B. Yuferov and F.I. Busol, Sov. Phys. Tech. Phys. **11** (1967) 1518.

[79] V.B. Yuferov and P.M. Kobzev, Sov. Phys. Tech. Phys. **14** (1969) 1261.

[80] V.B. Yuferov and P.M. Kobzev, Sov. Phys. Tech. Phys. **15** (1971) 2041.

[81] M.M. Menon, G.J. Laughon, R. Maingi, M.R. Wade, D.L. Hillis and M.A. Mahdavi, J. Vac. Sci. Technol. **A 13** (1995) 551.

[82] J. Kim, K.M. Schaubel and A.P. Colleraine, J. Vac. Sci. Technol. **A 8** (1990) 3084.

[83] J.H. Kamperschroer, M.B. Cropper, H.F. Dylla, V. Garzotto, L.E. Dudek, L.R. Grisham, G.D. Martin, T.E. O'Connor, T.N. Stevenson, A. von Halle, M.D. Williams and J. Kim, J. Vac. Sci. Technol. **A 8** (1990) 3079.

[84] T.H. Batzer, R.E. Patrick and W.R. Call, J. Vac. Sci. Technol. **18** (1981) 1125.

[85] M.P. Larin, Sov. Phys. Tech. Phys. **33** (1988) 455.

[86] E. Wallen, J. Vac. Sci. Technol. **A 14** (1996) 2916.

[87] J.C. Boissin, J.J. Thibault and H. Richardt, Le Vide **157** (1972) 103.

[88] J. Hengevoss and E.A. Trendelenburg, Vacuum **17** (1967) 495.

[89] J.J. Thibault, J.M. Disdier, G. Arnaud, J.C. Boissin and C.B. Hood, J. Vac. Sci. Technol. **18** (1981) 1140.

[90] P.A. Lessard, J. Vac. Sci. Technol. **A 7** (1989) 2373.

[91] R.C. Longsworth, Adv. Cryog. Eng. **23** (1978) 658.

[92] R.C. Longsworth and Y. Lahav, J. Vac. Sci. Technol. **A 5** (1987) 2646.

[93] H.C. Hseuh and H.A. Worwetz, J. Vac. Sci. Technol. **18** (1981) 1131.

[94] R.I. Shcherbachenko and V.N. Grigor'ev, Low Temp. Phys. **24** (1998) 831.

[95] B. Liu, J. Xie, J. Ren and X. Cui, J. Vac. Sci. Technol. **A 5** (1987) 2577.

[96] J.R. Coupland, D.P. Hammond, W. Bächler and H.H. Klein, J. Vac. Sci. Technol. **A 5** (1987) 2563.

[97] A.J. Kidnay, M.J. Hiza and P.F. Dickson, Adv. Cryog. Eng. **13** (1968) 397.

[98] C. Johannes, Adv. Cryog. Eng. **17** (1972) 213.

[99] B.P.M. Helvensteijn, A. Kashani, R.A. Wilcox and A.L. Spivak, Adv. Cryog. Eng. **39** (1994) 1561.

[100] B.P.M. Helvensteijn, A. Kashani and R.A. Wilcox, Adv. Cryog. Eng. **37** (1992) 1129.

[101] I. Vazquez, M.P. Russell, D.R. Smith and R. Radebaugh, Adv. Cryog. Eng. **33** (1988) 1013.

[102] R. Yanik, Vacuum **47** (1996) 205.

[103] H. Parish, Adv. Cryog. Eng. **35** (1990) 1541.

[104] K.M. Welch, B. Andeen, J.E. deRijke, C.A. Foster, M.H. Hablanian, R.C. Longsworth, W.E. Millikin, Y.T. Sasaki and C. Tzemos, J. Vac. Sci. Technol. **A 17** (1999) 3081.

[105] H.-J. Mundinger, H.U. Häfner, M. Mattern-Klosson, H.H. Klein and U. Timm, Vacuum **43** (1992) 545.

[106] M. Iseli, Fusion Eng. Design **54** (2001) 421.

[107] Chr. Day, Use of porous materials for cryopumping, *in*: H.S. Nalwa, *Handbook of Surfaces and Interfaces of Materials* (Academic Press, San Diego, 2001), vol. 5, p. 265.

[108] I. Özdemir and D. Perinić, J. Vac. Sci. Technol. **A 16** (1998) 2524.

[109] Chr. Day *et al*., Fusion Sci. Technol. **48** (2005) 29.

[110] Chr. Day and A. Schwenk-Ferrero, Vacuum **53** (1999) 253.

[111] Chr. Day et al., Vacuum **81** (2007) 738.

[112] Chr. Day, Colloids and Surfaces **A 187–188** (2001) 187.

[113] H.E. Nuss and I. Streuff, Vacuum **47** (1996) 391.

[114] W. Obert, C. Mayaux and G. Perinić, Adv. Cryog. Eng. **39** (1994) 1569.

[115] Y. Oka, T. Takanashi, R. Akiyama, O. Kaneko, K. Toi, H. Morimoto, M. Terashima and T. Kuroda, Fusion Eng. Design **31** (1996) 89.

[116] P. Lebrun, IEEE Trans. Appl. Supercond. **10** (2000) 1500.

[117] J. Miertusova, Vacuum **48** (1997) 751.

[118] H.C. Hseuh, R. Davis, D. Pate, L. Smart, R. Todd and D. Weiss, Vacuum **53** (1999) 347.

[119] H. Dombrowski, D. Grzonka, W. Hamsink, A. Khoukaz, T. Lister and R. Santo, Nucl. Instrum. Methods Phys. Res. **A 386** (1997) 228.

[120] Chr. Day *et al*., Fusion Eng. Design **58–59** (2001) 301.

[121] V. Hauer *et al*., Design of the ITER torus prototype cryopump, accepted for publication in Fusion Engineering and Design.

[122] M. Dremel *et al*., Adv. Cryog. Eng. **51** (2006) 583.

Bibliography

Vacuum technology in general

R.A. Haefer, *Kryo-Vakuumtechnik* (Springer, Berlin, 1981).

M. Wutz *et al*., *Handbuch Vakuumtechnik*, 8th ed. (Vieweg, Braunschweig, 2004).

J.M. Lafferty (Ed.), *Foundations of Vacuum Science and Technology* (Wiley, New York, 1998).

A. Roth, *Vacuum Technology*, 3rd ed. (North-Holland, Amsterdam, 1990).

J.F. O'Hanlon, *A User´s Guide to Vacuum Technology*, 3rd ed. (Wiley, Hoboken, 2003).

N.S. Harris, *Modern Vacuum Practice* (McGraw-Hill, London, 1989).

Cryopumps in particular

R.A. Haefer, *Cryopumping* (Clarendon Press, Oxford, 1989).

K.M. Welch, *Capture Pumping Technology*, 2nd ed. (North-Holland Elsevier, Amsterdam, 2001).

M.H. Hablanian, *High-Vacuum Technology*, 2nd ed. (Dekker, New York, 1997).

L.N. Rozanov, *Vacuum Technique* (Taylor & Francis, London, 2002).

Cryogenics

K.D. Timmerhaus and T.M. Flynn, *Cryogenic Process Engineering* (Plenum Press, New York, 1989).

R.F. Barron, *Cryogenic Systems*, 2nd ed. (Oxford University Press, New York, 1985).

J.G. Weisend II (Ed.), *Handbook of Cryogenic Engineering* (Taylor & Francis, Philadelphia, 1998).